

IEEE Copyright Notice

© 2019 IEEE. Personal use of this material is permitted. Permission from IEEE must be obtained for all other uses, in any current or future media, including reprinting/republishing this material for advertising or promotional purposes, creating new collective works, for resale or redistribution to servers or lists, or reuse of any copyrighted component of this work in other works.

Limited Feedback Designs for Machine-type Communications Exploiting User Cooperation

Jiho Song, *Member, IEEE*, Byungju Lee, *Member, IEEE*, Song Noh, *Member, IEEE*, and Jong-Ho Lee, *Member, IEEE*,

Abstract—Multiuser multiple-input multiple-output (MIMO) systems are a prime candidate for use in massive connection density in machine-type communication (MTC) networks. One of the key challenges of MTC networks is to obtain accurate channel state information (CSI) at the access point (AP) so that the spectral efficiency can be improved by enabling enhanced MIMO techniques. However, current communication mechanisms relying upon frequency division duplexing (FDD) might not fully support an enormous number of devices due to the rate-constrained limited feedback and the time-consuming scheduling architectures. In this paper, we propose a user cooperation-based limited feedback strategy to support high connection density in massive MTC networks. In the proposed algorithm, two close-in users share the quantized version of channel information in order to improve channel feedback accuracy. The cooperation process is performed without any transmitter interventions (i.e., in a grant-free manner) to satisfy the low-latency requirement that is vital for MTC services. Moreover, based on the sum-rate throughput analysis, we develop an adaptive cooperation algorithm with a view to activating/deactivating the user cooperation mode according to channel and network conditions.

I. INTRODUCTION

INTERNET of things (IoT), which refers to the connected future world in which every mobile device and machines are linked to the internet via wireless link, has received attention from both academia and industry in recent years [1]. IoT enables a wide range of unprecedented services such as autonomous driving, smart home/factory, and factory automation, just to name a few [2]. Massive connectivity is one of the most important requirements of a fully connected IoT society [3], [4]. In accordance with this trend, the international telecommunication union (ITU) defined massive machine-type communication (mMTC) as one representative service category.¹ In mMTC networks, data communications may occur between an MTC device and a server or directly between MTC devices [6]. It is of considerable importance to support high connection density with limited resources because the number of devices is at least two orders of magnitude higher than current human-centric communication.

J. Song is with the School of Electrical Engineering, University of Ulsan, Ulsan, South Korea (e-mail: jihosong@ulsan.ac.kr).

B. Lee (*corresponding author*) is with Samsung Research, Seoul, Korea (email: byungjulee1730@gmail.com).

S. Noh is with the Department of Information and Telecommunication Engineering, Incheon University, Incheon, South Korea (email: songnoh@inu.ac.kr).

J.-H. Lee is with the School of Electronic Engineering, Soongsil University, Seoul, South Korea (e-mail: jongho.lee@ssu.ac.kr).

This work was supported by the 2018 Research Fund of University of Ulsan.

¹Three representative service categories include enhanced mobile broadband (eMBB), ultra-reliable and low latency communication (uRLLC), and massive machine-type communication (mMTC) [5].

From a technological standpoint, enormous number of devices in mMTC networks can be used to exploit full benefit of multiuser MIMO. It is essential to have high-resolution channel state information (CSI) at the access point (AP) to exploit multiuser diversity gain [7], [8]. In most current cellular systems relying upon frequency division duplexing (FDD), the quantized CSI is communicated to the AP via a rate-constrained feedback link [9]–[11]. One challenge of feedback-assisted multiuser systems is that low-resolution CSI overrides the multiuser diversity gain because the signal-to-interference-plus-noise ratio (SINR) is limited due to the channel quantization error [12], [13]. In the feedback-assisted multiuser systems, the rate-constrained feedback mechanism is the biggest obstacle to supporting a massive number of devices on an MTC network.

Antenna combining techniques, e.g., *quantization-based combining* (QBC) [14], has been proposed to obtain high-resolution CSI. A key feature of the QBC is that receive antennas are combined to generate an effective channel that can be quantized accurately. Employing more antennas would enhance the quantization performance. However, direct application of antenna combining techniques for mMTC is infeasible since it is difficult to employ multiple antenna elements due to the strict budget constraints on small-scale devices. In this paper, we develop a cooperative feedback strategy to obtain an additional spatial dimension for the antenna combining process without imposing an additional burden on mMTC devices.

Recently, multiuser systems incorporating user cooperation algorithms have been proposed [15], [16]. In [15], the user in the cooperative link helps other adjacent users by forwarding adjacent users' information while achieving its own quality of service (QoS). In [16], the users in the cooperative link exchange their CSI via device-to-device (D2D) communications. The users can compute a more appropriate precoder at the user side because CSI exchange allows users to obtain the global CSI. However, since the number of users² for the mMTC network is much larger than that of current human-centric communication, it is not feasible to exchange CSI with all the other users. Therefore, it is important to develop solutions with minimal overhead for feedback and/or cooperative links.

The aim of this paper is to develop user cooperation strategies for an mMTC network allowing only point-to-point CSI exchange between close-in users. In order to obtain high-resolution CSI with a minimal burden on the user cooperation framework, few bits are exploited to exchange CSI. To the best of our knowledge, a user cooperation strategy designed

²The users can be any kinds of machines, devices, and mobile users.

to reduce channel quantization error has been proposed here for the first time. The main contributions of this paper are summarized as follows:

- *Cooperative limited feedback*: Adjacent users are connected to a cooperation link and these users are considered one cooperation unit (CU). Each user in CU shares the other user's *local* channel information (i.e., *local* channel direction information (CDI) and channel quality indicator (CQI)). CSI sharing is only allowed between users in a CU. Each user generates the *global* channel information required for downlink transmission (i.e., *global* CDI and CQI) using its own channel information and the *local* channel information received from an adjacent user. After exchanging each other's *global* CQI, the user having larger *global* CQI is assigned as the main user (MU) and the other user is assigned as an assistant user (AU). The AU acts as an assistant for MU by allowing MU to use its receive antennas to construct the *global* CDI more precisely. The MU only feeds back the *global* CSI so that the AP perceives the MU as the sole active user, while the AU is transparent to the AP. In the data transmission phase, both the MU and AU receive data information from the AP and then the AU forwards the received signal to the MU. The channel feedback accuracy of the MU is improved due to the virtue of exploiting AU resources.
- *Automatic role assignment*: Identification of the MU and AU is an important issue since only the spectral efficiency of the MU can be increased by sacrificing the resources of the AU. In the proposed algorithm, the cooperation process between users is designed to occur without transmitter intervention (i.e., a grant-free environment) through an active decision process. An important issue behind this active decision process is the motivation for participating in cooperative communication as the AU.³ Under a grant-free environment, the AP regards the MU as the sole user and this identification process is transparent to the AP.
- *Adaptive cooperative feedback*: If cooperative feedback is activated, the number of active users is reduced by half because two users are combined as a single CU to obtain high-resolution CSI. Unless a massive number of users are active in the mMTC network, the cooperative feedback strategy might not be an effective solution because the multiuser diversity gain is highly limited in a small-user regime. For this reason, effective allocation of limited multiuser resources is required to obtain accurate CSI without loss of multiuser diversity gain. We analyze the sum-rate throughput of the multiuser MIMO systems relying upon the proposed cooperation algorithm. Based on the analytical studies, we develop cooperation mode switching criteria to activate/deactivate the cooperation mode according to channel and network conditions.

³One possible option can be the social relationship between users [16]. If users have a close relationship in the social domain, users can readily help each other by using their own resources for cooperative feedback. Other possible scenario can be the cooperation between different devices in each user. Alternatively, an artificial intelligence (AI)-based and/or game-theoretic approach can be applied in identifying the MU and AU and this would be an interesting future research topic.

In Section II, we briefly introduce a multiuser MIMO system and review a user selection algorithm. In Section III, we present the proposed cooperative feedback algorithm. An adaptive cooperation algorithm is developed based on analytical studies on sum-rate throughput in Section IV. In Section V, we present numerical results to verify the performance of the proposed scheme. We conclude the paper in Section VI.

Throughout this paper, \mathbb{C} denotes the field of complex numbers, $\mathcal{CN}(m, \sigma^2)$ denotes the complex normal distribution with mean m and variance σ^2 , $\mathbf{0}_{a,b}$ is the $a \times b$ all zeros matrix, $\mathbf{1}_{a,b}$ is the $a \times b$ all ones matrix, \mathbf{I}_M is the $M \times M$ identity matrix, χ^2 is the Chi-squared random variable, $\beta(\cdot, \cdot)$ is the Beta-distributed random variable, $\mathbf{B}(\cdot, \cdot)$ is the Beta function, $\Gamma(\cdot)$ is the gamma function, $\binom{n}{k}$ is the binomial coefficient, $(z)_k$ is the Pochmann symbol, $\lceil \cdot \rceil$ is the ceiling function, $\mathbb{E}[\cdot]$ is the expectation operator, $\mathbb{1}$ is the indicator function, $\|\cdot\|_p$ is the p -norm, and $[\mathbf{a}]_\ell$ is the ℓ -th element of the column vector \mathbf{a} . Also, $\mathbf{A}_{:,m}$, \mathbf{A}^\dagger , \mathbf{A}^H , $\text{Tr}(\mathbf{A})$, and $\mathbf{A}_{a,b}$ denote m -th column vector, pseudo-inverse, conjugate transpose, trace, and (a, b) -th entry of the matrix \mathbf{A} , respectively.

II. SYSTEM MODEL AND BACKGROUND

We briefly review the FDD-based multiuser MIMO systems. We first present the system model and then discuss *antenna combining*-based limited feedback. An overview of conventional multiuser MIMO systems is depicted in Fig. 1(a).

A. System Model

We consider multiuser MIMO systems employing M transmit antennas at the AP and N receive antennas at each of K users. Assuming a block-fading channel, an input-output expression for the k -th user⁴ is defined as

$$y_k = \mathbf{z}_k^H (\sqrt{\rho} \mathbf{H}_k \mathbf{x} + \mathbf{n}_k), \quad (1)$$

where $y_k \in \mathbb{C}$ is the received baseband signal, ρ is the signal-to-noise ratio (SNR), $\mathbf{z}_k \in \mathbb{C}^N$ is the unit-norm combiner,

$$\mathbf{H}_k \doteq [\mathbf{h}_k^1, \dots, \mathbf{h}_k^N]^H \in \mathbb{C}^{N \times M} \quad (2)$$

is the MIMO channel matrix, $\mathbf{h}_k^n \in \mathbb{C}^M$ is the channel vector between the AP and the n -th receive antenna consisting of independent and identically distributed (i.i.d.) entries following $\mathcal{CN}(0, 1)$, $\mathbf{x} \in \mathbb{C}^M$ is the transmit signal vector (with the power constraint $\mathbb{E}[\|\mathbf{x}\|_2^2] \leq 1$), and $\mathbf{n}_k \in \mathbb{C}^N$ is the additive noise vector with entries following $\mathcal{CN}(0, 1)$.

We consider a single layer data transmission for each user. The transmit signal vector is rewritten as $\mathbf{x} \doteq \mathbf{F}\mathbf{s}$, where

$$\mathbf{F} = \frac{1}{\sqrt{M}} [\mathbf{f}_1, \dots, \mathbf{f}_M] \in \mathbb{C}^{M \times M}$$

is the precoder and $\mathbf{s} = [s_1, \dots, s_M]^T \in \mathbb{C}^M$ is the transmit symbol vector. Note that $\mathbf{f}_m \in \mathbb{C}^M$ and $s_m \in \mathbb{C}$ denote the transmit beamformer and the data stream for the m -th scheduled user with the power constraints $\|\mathbf{f}_m\|_2^2 = 1$ and $\mathbb{E}[|s_m|^2] \leq 1$.

In FDD-based cellular systems, an AP obtains channel information through receiver feedback from each user. In

⁴The user index is subscripted and the set of user indices in the network is written by $\mathcal{K} = \{1, \dots, K\}$.

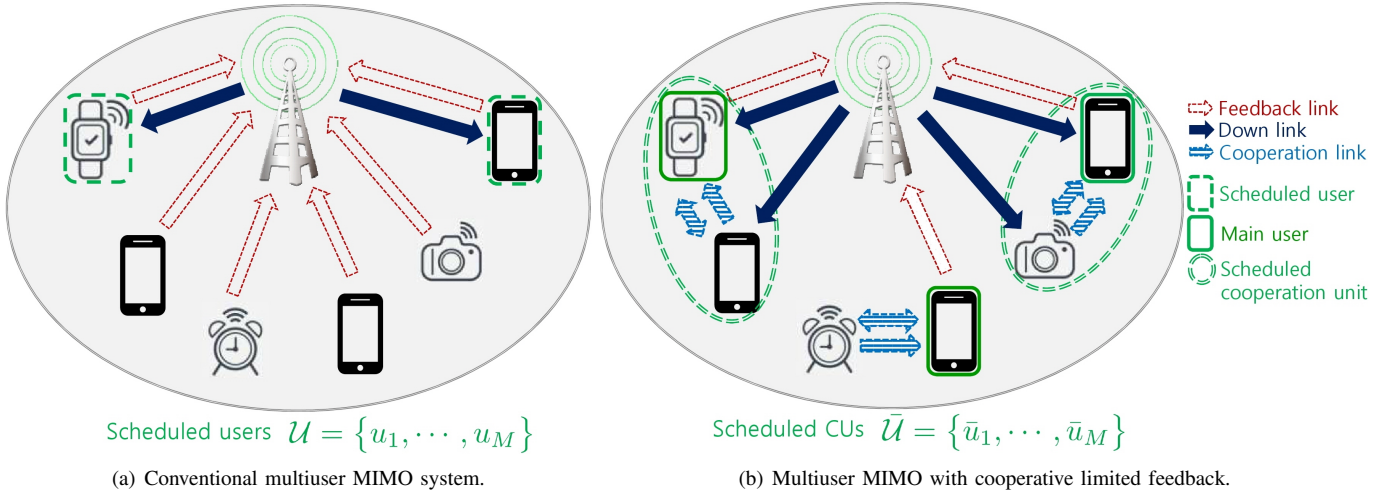


Fig. 1. An overview of multiuser MIMO systems.

feedback-assisted MIMO architectures, channel vectors are quantized using the predefined codebook

$$\mathcal{C} \doteq \{\mathbf{c}^1, \dots, \mathbf{c}^Q\}. \quad (3)$$

where $Q = 2^B$ is the number of codewords in the *global* codebook. To facilitate the multiuser signaling framework, the quantized channel information is fed back to the AP via a rate-constrained $B = \lceil \log_2 Q \rceil$ -bit feedback link.

We employ the opportunistic random beamforming approach that utilizes a set of unitary matrices to construct the *global* codebook [7], [17]. Similar to the LTE-Advanced codebooks in [18], [19], exploiting more sets of unitary matrices (i.e., oversampled discrete Fourier transform (DFT) codebook) enables the AP to obtain high-resolution CSI. However, an ultra low-latency requirement for MTC services restricts the use of large codebooks. Assuming an intensely rate-constrained feedback link, we consider M codewords for channel feedback and beamforming, meaning that the number of codewords equals to the number of transmit antennas. If only M codewords are allowed for CSI quantization, it would be optimal to consider a set of orthonormal vectors for random beamforming [20]. We use a single unitary matrix $\mathbf{C} \doteq [\mathbf{c}^1, \dots, \mathbf{c}^M]$ for defining codewords according to $\mathbf{c}^m \doteq \mathbf{C}_{:,m}$.

B. QBC-based Limited Feedback for Multiuser MIMO

One major issue of the feedback architecture using M codewords is that the channel quantization performance is expected to be poor in a single receive antenna scenario. When multiple receive antennas are available, antenna combining techniques can be applied to enhance the channel quantization performance [14], [21]. In this paper, we consider a QBC-based antenna combining algorithm [14]. The objective of the QBC algorithm is to compute an effective channel vector that can be quantized accurately using a small-sized codebook. For a given target codeword \mathbf{c}^m , the receive combiner $\bar{\mathbf{z}}_{k|m}$ is computed such that a cross-correlation between the effective channel

$$\bar{\mathbf{h}}_{k|m}^{\text{eff}} = \mathbf{H}_k^H \bar{\mathbf{z}}_{k|m} \quad (4)$$

and the target codeword is maximized. As discussed in [14], the effective channel that maximizes the cross-correlation is obtained by projecting \mathbf{c}^m onto the channel subspace such that

$$\mathbf{c}^{\text{proj},m} = \frac{[\mathbf{q}^1, \dots, \mathbf{q}^N][\mathbf{q}^1, \dots, \mathbf{q}^N]^H \mathbf{c}^m}{\|[\mathbf{q}^1, \dots, \mathbf{q}^N][\mathbf{q}^1, \dots, \mathbf{q}^N]^H \mathbf{c}^m\|_2} \in \mathbb{C}^M, \quad (5)$$

where \mathbf{q}^n is the orthonormal basis that spans \mathbf{H}_k . Using the QBC algorithm, the receive combiner $\bar{\mathbf{u}}_{k|m}$, which satisfies $\mathbf{H}_k^H \bar{\mathbf{u}}_{k|m} = \mathbf{c}^{\text{proj},m}$, can be computed by multiplying the pseudo-inverse of the channel matrix such as

$$(\mathbf{H}_k \mathbf{H}_k^H)^{-1} \mathbf{H}_k \mathbf{H}_k^H \bar{\mathbf{u}}_{k|m} = (\mathbf{H}_k \mathbf{H}_k^H)^{-1} \mathbf{H}_k \mathbf{c}^{\text{proj},m}.$$

Finally, the unit-norm combiner is computed according to

$$\bar{\mathbf{z}}_{k|m} \doteq \frac{\bar{\mathbf{u}}_{k|m}}{\|\bar{\mathbf{u}}_{k|m}\|_2} = \frac{(\mathbf{H}_k \mathbf{H}_k^H)^{-1} \mathbf{H}_k \mathbf{c}^{\text{proj},m}}{\|(\mathbf{H}_k \mathbf{H}_k^H)^{-1} \mathbf{H}_k \mathbf{c}^{\text{proj},m}\|_2} \in \mathbb{C}^N. \quad (6)$$

Assuming the user k is scheduled to use the m -th beamformer (codeword), the received signal is written by

$$\begin{aligned} y_{k|m} &= \sqrt{\rho} \bar{\mathbf{z}}_{k|m}^H \mathbf{H}_k \left(\frac{[\mathbf{c}^1, \dots, \mathbf{c}^M]}{\sqrt{M}} \right) \mathbf{s} + \bar{\mathbf{z}}_{k|m}^H \mathbf{n}_k \\ &= \sqrt{\frac{\rho}{M}} \left((\bar{\mathbf{h}}_{k|m}^{\text{eff}})^H \mathbf{c}^m s_m + \sum_{\ell=1, \ell \neq m}^M (\bar{\mathbf{h}}_{k|m}^{\text{eff}})^H \mathbf{c}^\ell s_\ell \right) + \bar{n}_{k|m}, \end{aligned} \quad (7)$$

because the m -th beamformer is identical to the m -th codeword such that $\mathbf{f}_m = \mathbf{c}^m$ in our random beamforming architecture. Notice that $\bar{n}_{k|m} \doteq \bar{\mathbf{z}}_{k|m}^H \mathbf{n}_k \sim \mathcal{CN}(0, 1)$ denotes the combined noise. The SINR of the k -th user is then defined by⁵

$$\bar{\gamma}_{k|m} \doteq \frac{|(\bar{\mathbf{h}}_{k|m}^{\text{eff}})^H \mathbf{c}^m|^2}{\frac{M}{\rho} + \sum_{\ell=1, \ell \neq m}^M |(\bar{\mathbf{h}}_{k|m}^{\text{eff}})^H \mathbf{c}^\ell|^2}. \quad (8)$$

From among M beamformers $\{\mathbf{c}^1, \dots, \mathbf{c}^M\}$, each user (e.g.,

⁵In our beamforming scenario exploiting a single unitary matrix, the SINR can be computed at the receiver side because the k -th user knows all the transmit beamformers, i.e., \mathbf{c}^ℓ , $\ell \neq k$, assigned for other users. The SINR can be regarded as CQI that quantifies the quality of each transmission layer.

k -th user) selects a single beamformer

$$\bar{\mathbf{v}}_k \doteq \mathbf{c}^{\hat{m}} \quad (9)$$

that maximizes the SINR according to $\bar{\gamma}_k = \bar{\gamma}_{k|\hat{m}}$, where the index of the selected codeword is $\hat{m} \doteq \arg \max_m \bar{\gamma}_{k|m}$, and the selected combiner is⁶ $\bar{\mathbf{z}}_k = \bar{\mathbf{z}}_{k|\hat{m}}$. We call the selected beamformer $\bar{\mathbf{v}}_k$ *global* CDI and the selected SINR $\bar{\gamma}_k$ *global* CQI. In this paper, we focus on quantizing the CDI and refer to [22] and the references therein for quantizing the CQI. We assume that the index of the quantized CDI is fed back via an error-free B -bit feedback link and the unquantized CQI can be communicated to the AP.

Finally, we refer to the user selection algorithm in [22] to schedule/select M users from among $K \gg M$ users such that

$$\mathcal{U} = \{u^1, \dots, u^M\},$$

where u^m denotes the scheduled user exploiting the m -th codeword \mathbf{c}^m . The m -th scheduled user is given by

$$u^m \doteq \arg \max_{k \in \mathcal{K}^m} \gamma_k,$$

where \mathcal{K}^m denotes the set of indices of users who choose \mathbf{c}^m as their *global* CDI. It should be noted that the multiuser diversity gain from user selection plays a significant role in improving the sum-rate throughput and it grows like $M \log_2(\log K)$ under the perfect CSI assumption at the AP [7], [23].

Despite the advantage, it has some obstacles that hinder the direct application of conventional multiuser systems to mMTC. First, the channel quantization error overrides the multiuser diversity gain. In feedback-assisted FDD architectures, multiuser systems become interference-limited due to unsuppressed quantization error. The sum-rate is thus upper bounded even though the SNR goes to infinity [12], [13]. Second, a large number of devices imposes a heavy burden on the initial access architecture of cellular networks. In 5G new radio (NR), there are a limited number of physical-layer cell identities [4]. Since there is no specific collision avoidance procedure, a massive number of access attempts can cause severe congestions that accompany the increase in transmission latency [3]. Even assuming congestion-free scenarios, the sum-rate growth in a large-user regime $K \gg M$ has slowed because the sum-rate grows in a double-logarithmical fashion [23], [24].

III. COOPERATIVE LIMITED FEEDBACK ARCHITECTURE

One of the key challenges in developing feedback-assisted multiuser systems for mMTC is to obtain accurate CSI at the AP while overcoming the following restrictions:

- Ultra low-latency requirement for mMTC restricts the use of large codebook and this make it difficult to achieve robust channel quantization performance.
- Considering the strict budget constraints of small-scale devices, it is not practical to employ a multitude of antenna elements for the antenna combining.

In QBC, the resolution of an effective channel increases as the spatial dimensions of a channel matrix for an antenna

combining increases [14]. In this paper, we propose user cooperation strategies to obtain high-resolution CSI while limiting the number of antenna elements at the receiver. The main feature of the proposed algorithm is that users in a CU employ an additional spatial dimension for the antenna combining by allowing a limited amount of CSI exchange. The key difference between the conventional system in Fig. 1(a) and the proposed system in Fig. 1(b) is the existence of the cooperation link. We assume that the quantized version of CSI can be exchanged between close-in users by using the Wi-Fi peer-to-peer sidelink, as presented in [25].

Before presenting the cooperative limited feedback algorithm, we pause to provide supporting details behind the variables in the proposed cooperative feedback architecture:

- The term *global* is used to designate the variables and signal processing operations within CU, while the term *local* is used to designate the variables and signal processing operations within AU.
- The bar symbol $\bar{\cdot}$ will be used to highlight variables corresponding to the *global* signal processing operation.
- The tilde symbol $\tilde{\cdot}$ will be used to highlight variables corresponding to the downlink transmission.

We present the details of the cooperative feedback algorithm based on the assumption that two close-in users have already been combined as a single CU⁷ according to $\{a, b\}$.

1) **Local CSI acquisition:** An aim of this step is to compute *local* CSI that will be used to increase spatial dimensions of the partner's channel matrix. The quantized version of *local* CSI is transferred to its partner via a cooperation link.

One viable approach to achieve reduction of both *local* CSI quantization error and cooperation link overhead is to share only a single effective channel vector that is combined based on the QBC algorithm [14]. The combined channel is quantized using the random vector quantization (RVQ) codebook

$$\mathcal{D} \doteq \{\mathbf{d}^1, \dots, \mathbf{d}^{Q^{\text{cl}}}\}, \quad (10)$$

which consists of $Q^{\text{cl}} = 2^{B^{\text{cl}}}$ codewords. The distance of the cooperation link is much shorter than that of the feedback link. The cooperation link would be subject to less stringent overhead constraints compared to that for the feedback link such that $B^{\text{cl}} \gg B$.

First, user $k \in \{a, b\}$ in the CU computes a virtual vector

$$\mathbf{h}_{k|q}^{\text{virt}} \doteq \mathbf{H}_k^H \mathbf{z}_{k|q} \quad (11)$$

that can be quantized more accurately using a target codeword $\mathbf{d}^q \in \mathcal{D}$, where the *local* combiner $\mathbf{z}_{k|q} \in \mathbb{C}^N$ and the projected codeword $\mathbf{d}^{\text{proj},q} \in \mathbb{C}^M$, needed for the *local* channel combining, are computed using similar method in (5) and (6).

Second, each user selects a *local* codeword that maximizes the cross-correlation of the normalized virtual channel vector and the codeword, i.e.,

$$\cos^2 \phi_{k|q} = |(\mathbf{d}^q)^H \mathbf{h}_{k|q}^{\text{virt}} / \|\mathbf{h}_{k|q}^{\text{virt}}\|_2|^2, \quad (12)$$

⁶For the sake of simplicity, the index of the selected codeword is dropped for the rest of the sections.

⁷Developing a user grouping algorithm for holding two users together to form CU and/or considering a coalition of more than two users in a CU would be an interesting future research topic.

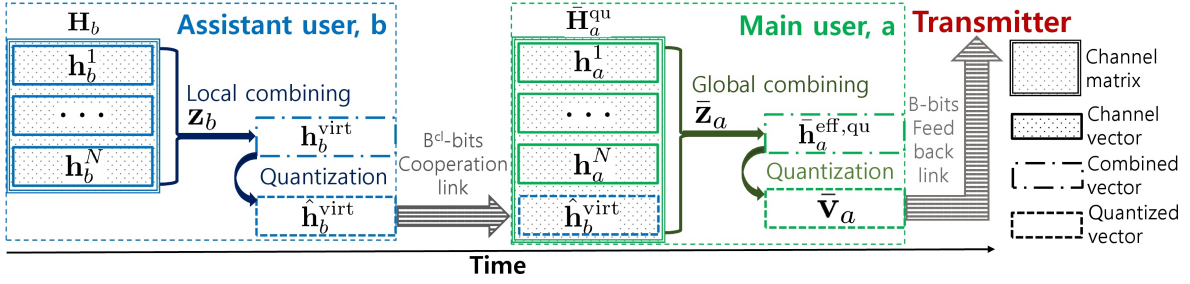


Fig. 2. An overview of *global* and *local* combining processes.

where $\phi_{k|q}$ is the difference in angle. We call the selected codeword *local* CDI and its corresponding cross-correlation coefficient *local* CQI. The *local* CDI and CQI are given by

$$(\mathbf{v}_k, \tau_k) \doteq (\mathbf{d}^{\hat{q}}, \|\mathbf{h}_{k|\hat{q}}^{\text{virt}}\|_2 \cos \phi_{k|\hat{q}}), \quad (13)$$

where the index of the selected codeword is

$$\hat{q} = \arg \max_{q \in \{1, \dots, Q^{\text{cl}}\}} \cos^2 \phi_{k|q}.$$

Under the assumption the index of the selected codeword is dropped, the selected *local* combiner, the virtual channel vector, and the difference in angle can be rewritten as

$$(\mathbf{z}_k, \mathbf{h}_k^{\text{virt}}, \phi_k) \doteq (\mathbf{z}_{k|\hat{q}}, \mathbf{h}_{k|\hat{q}}^{\text{virt}}, \phi_{k|\hat{q}}). \quad (14)$$

The quantized virtual channel vector is then defined with the *local* CDI and CQI according to

$$\hat{\mathbf{h}}_k^{\text{virt}} \doteq \tau_k \mathbf{v}_k = \|\mathbf{h}_k^{\text{virt}}\|_2 \cos \phi_k \mathbf{v}_k. \quad (15)$$

Finally, users in the CU exchange the *local* CDI and CQI, i.e., quantized virtual channel vector $\hat{\mathbf{h}}_k^{\text{virt}}$ in (15), with its cooperation partner via a B^{cl} -bits cooperation link. The *local* CDI and CQI will be included in a *global* channel matrix of its cooperation partner. The *local* combining and quantization processes are depicted in the left side of Fig. 2.

2) **Global CSI acquisition & Role assignment:** An aim of this step is to compute *global* channel information and to assign the role of MU and AU. The *global* CSI will be fed back to the AP.

First, each user constructs a *global* channel matrix

$$\bar{\mathbf{H}}_k^{\text{qu}} \doteq \begin{bmatrix} \mathbf{H}_k \\ (\hat{\mathbf{h}}_{k^c}^{\text{virt}})^H \end{bmatrix} \in \mathbb{C}^{(N+1) \times M}, \quad (16)$$

which includes one's own channel matrix \mathbf{H}_k and the quantized virtual channel vector $\hat{\mathbf{h}}_{k^c}^{\text{virt}}$ from a cooperation partner, where $k^c \in \{a, b\} \setminus \{k\}$. Each user regards the virtual channel vector as an additional channel vector between the AP and the virtual antenna element at the receiver. Assuming oneself is selected as MU, each user computes the *global* effective channel vector

$$\bar{\mathbf{h}}_{k|m}^{\text{eff,qu}} = (\bar{\mathbf{H}}_k^{\text{qu}})^H \bar{\mathbf{z}}_{k|m} \quad (17)$$

that can be quantized accurately with a target codeword $\mathbf{c}^m \in \mathcal{C}$. The *global* combiner $\bar{\mathbf{z}}_{k|m} \in \mathbb{C}^{N+1}$ is computed using the combining method in (5) and (6). The difference with the combining process in (11) is that the rank of the channel matrix and the dimension of the combiner are increased to

$N + 1$.

Second, each user selects a single *global* codeword that maximizes the SINR

$$\bar{\gamma}_{k|m} \doteq \frac{|(\bar{\mathbf{h}}_{k|m}^{\text{eff,qu}})^H \mathbf{c}^m|^2}{\frac{M}{\rho} + \sum_{\ell=1, \ell \neq m}^M |(\bar{\mathbf{h}}_{k|m}^{\text{eff,qu}})^H \mathbf{c}^\ell|^2}.$$

We call the selected codeword *global* CDI and its corresponding SINR *global* CQI. The *global* CDI and CQI are

$$(\bar{\mathbf{v}}_k, \bar{\gamma}_k) \doteq (\mathbf{c}^{\hat{m}}, \bar{\gamma}_{k|\hat{m}}), \quad (18)$$

where the index of the selected codeword is $\hat{m} \doteq \arg \max_m \bar{\gamma}_{k|m}$. Assuming the index of the selected codeword is dropped, the selected *global* combiner and the effective channel vector are rewritten according to

$$(\bar{\mathbf{z}}_k, \bar{\mathbf{h}}_k^{\text{eff,qu}}) \doteq (\bar{\mathbf{z}}_{k|\hat{m}}, \bar{\mathbf{h}}_{k|\hat{m}}^{\text{eff,qu}}). \quad (19)$$

Third, users in the CU exchange their *global* CQIs with cooperating users via a cooperation link to determine who's best for maximizing the data-rate throughput. The user having a larger CQI is assigned to MU and the unselected user is assigned to AU. The role assignment are made at the beginning of the transmission frame and will continue for the duration of the channel coherence time. We assume that the a -th (odd number indexed) user is assigned to MU and the b -th (even number indexed $b = a + 1$) user is assigned to AU. The set of indices of MUs is then written by $\bar{\mathcal{K}} = \{1, 3, \dots, K - 1\}$.

Finally, MU only transmits the *global* CSI to the AP via a feedback link. The number of active users in the network is thus reduced by half $|\bar{\mathcal{K}}| = K/2$. The *global* combining and quantization processes are depicted in the right side of Fig. 2.

3) **User scheduling:** After collecting *global* CDI and CQI from $K/2$ MUs, the AP schedules M MUs such that

$$\bar{\mathcal{U}} = \{\bar{u}^1, \dots, \bar{u}^M\},$$

where \bar{u}^m denotes the scheduled MU exploiting the m -th codeword \mathbf{c}^m . The m -th scheduled MU is given by

$$\bar{u}^m = \arg \max_{k \in \bar{\mathcal{U}}^m} \bar{\gamma}_k,$$

where $\bar{\mathcal{U}}^m$ denotes the set of indices of MUs who choose \mathbf{c}^m as their *global* CDI.

Algorithm 1 Cooperative feedback algorithm

Step 1) Local CSI acquisition1: Compute *local* combiner and virtual channel vector

$$\mathbf{z}_{k|q} = \frac{(\mathbf{H}_k \mathbf{H}_k^H)^{-1} \mathbf{H}_k \mathbf{d}^{\text{proj},q}}{\|(\mathbf{H}_k \mathbf{H}_k^H)^{-1} \mathbf{H}_k \mathbf{d}^{\text{proj},q}\|_2}, \quad \mathbf{h}_{k|q}^{\text{virt}} = \mathbf{H}_k^H \mathbf{z}_{k|q}$$

2: Select *local* CDI and CQI (\mathbf{v}_k, τ_k) 3: Exchange *local* CDI and CQI $\hat{\mathbf{h}}_k^{\text{virt}} = \tau_k \mathbf{v}_k$ **Step 2) Global CSI acquisition & Role assignment**4: Construct *global* channel matrix $\bar{\mathbf{H}}_k^{\text{qu}} = [\mathbf{H}_k^H, \hat{\mathbf{h}}_k^{\text{virt}}]^H$ 5: Compute *global* combiner and effective channel vector

$$\bar{\mathbf{z}}_{k|m} = \frac{(\bar{\mathbf{H}}_k^{\text{qu}} (\bar{\mathbf{H}}_k^{\text{qu}})^H)^{-1} \bar{\mathbf{H}}_k^{\text{qu}} \mathbf{c}^{\text{proj},m}}{\|(\bar{\mathbf{H}}_k^{\text{qu}} (\bar{\mathbf{H}}_k^{\text{qu}})^H)^{-1} \bar{\mathbf{H}}_k^{\text{qu}} \mathbf{c}^{\text{proj},m}\|_2},$$

$$\bar{\mathbf{h}}_{k|m}^{\text{eff,qu}} = (\bar{\mathbf{H}}_k^{\text{qu}})^H \bar{\mathbf{z}}_{k|m}$$

6: Select *global* CDI and CQI $(\bar{\mathbf{v}}_k, \bar{\gamma}_k)$ 7: Exchange *global* CQI8: Assign MU having a larger *global* CQI9: MU reports *global* CDI and CQI to the AP**Step 3) User scheduling**10: Schedule M MUs $\bar{\mathcal{U}} = \{\bar{u}^1, \dots, \bar{u}^M\}$ **Step 4) Post-signal processing**11: Save received signals \mathbf{y}_k 12: AU combines received signals $y_b = \mathbf{z}_b^H \mathbf{y}_b$ 13: AU reports y_b to MU14: MU obtains virtual received signals $\bar{\mathbf{y}}_a = [\mathbf{y}_a^T, y_b^T]^T$ 15: MU combines received signals $\bar{y}_{a|m} = \bar{\mathbf{z}}_{a|m}^H \bar{\mathbf{y}}_a$

4) **Post-signal processing:** An aim of this step is to decode the received signals⁸

$$\mathbf{y}_k = \sqrt{\rho} \mathbf{H}_k \mathbf{x} + \mathbf{n}_k \in \mathbb{C}^N, \quad k \in \{a, b\}. \quad (20)$$

First, AU combines the received signal with the *local* combiner \mathbf{z}_b such as

$$y_b = \sqrt{\rho} \mathbf{z}_b^H \mathbf{H}_b \mathbf{x} + \mathbf{z}_b^H \mathbf{n}_b = \sqrt{\rho} (\mathbf{h}_b^{\text{virt}})^H \mathbf{x} + n_b \in \mathbb{C}, \quad (21)$$

where $\mathbf{h}_b^{\text{virt}}$ is the unquantized virtual channel vector in (14). Second, the combined signal y_b is passed from AU to MU. Then, the MU constructs the *global* signal vector

$$\bar{\mathbf{y}}_a = \begin{bmatrix} \mathbf{y}_a \\ y_b \end{bmatrix} = \sqrt{\rho} \begin{bmatrix} \mathbf{H}_a \\ (\mathbf{h}_b^{\text{virt}})^H \end{bmatrix} \mathbf{x} + \begin{bmatrix} \mathbf{n}_a \\ n_b \end{bmatrix} = \sqrt{\rho} \bar{\mathbf{H}}_a \mathbf{x} + \bar{\mathbf{n}}_a \in \mathbb{C}^{N+1}, \quad (22)$$

where the *global* channel matrix corresponding to downlink transmission (downlink channel matrix) is defined by

$$\bar{\mathbf{H}}_a \doteq \begin{bmatrix} \mathbf{H}_a \\ (\mathbf{h}_b^{\text{virt}})^H \end{bmatrix} \in \mathbb{C}^{(N+1) \times M}, \quad (23)$$

and the *global* noise vector is $\bar{\mathbf{n}}_a \doteq [\mathbf{n}_a^T, n_b^T]^T \in \mathbb{C}^{N+1}$. Finally, the MU combines the *global* signal vector with the *global* combiner according to

$$\bar{y}_{a|m} = \bar{\mathbf{z}}_{a|m}^H \bar{\mathbf{y}}_a \in \mathbb{C}. \quad (24)$$

The detailed steps of the proposed algorithm are presented in Algorithm 1 and important variables are written in Table I.

⁸A memory in the receiver allows retention of received signals. The post-signal processing has no effect on a variation of the sum-rates because this process is conducted using the received signals stored in memory.

TABLE I
SUMMARY OF IMPORTANT VARIABLES

<i>Local</i>	Assistant user	$b \in \{2, 4, \dots, K\}$	
	Channel matrix	$\mathbf{H}_b = [\mathbf{h}_b^1, \dots, \mathbf{h}_b^N]^H$	(2)
	Codeword	$\mathbf{d}^q \in \mathcal{D}$	(10)
	Codebook size	$ \mathcal{D} = 2^{B^{\text{cl}}} = Q^{\text{cl}}$	(10)
	Combiner	$\mathbf{z}_{b q}$	(6)
	Virtual vector	$\mathbf{h}_{b q}^{\text{virt}} = \mathbf{H}_b^H \mathbf{z}_{b q}$	(11)
	CDI and CQI	(\mathbf{v}_b, τ_b)	(13)
	Quantized vector	$\hat{\mathbf{h}}_b^{\text{virt}} = \tau_b \mathbf{v}_b$	(15)
	<i>Global</i>	Main user	$a \in \{1, 3, \dots, K-1\}$
Channel matrix		$\bar{\mathbf{H}}_a^{\text{qu}} = [\mathbf{H}_a^H, \hat{\mathbf{h}}_b^{\text{virt}}]^H$	(16)
Codeword		$\mathbf{c}^m \in \mathcal{C}$	(3)
Codebook size		$ \mathcal{C} = 2^B = M$	(3)
Combiner		$\bar{\mathbf{z}}_{a m}$	(6)
Effective vector		$\bar{\mathbf{h}}_{a m}^{\text{eff,qu}} = (\bar{\mathbf{H}}_a^{\text{qu}})^H \bar{\mathbf{z}}_{a m}$	(17)
CDI and CQI		$(\bar{\mathbf{v}}_a, \bar{\gamma}_a)$	(18)

IV. ADAPTIVE COOPERATION ALGORITHM

The proposed cooperative feedback algorithm exploits some multiuser resources to improve channel quantization performance. High-resolution CSI can be obtained because more antenna elements (spatial dimensions) are used for *global* antenna combining. However, the proposed approach would restrict options that could be used to improve a network throughput due to the following reasons: First, the squared norm of the *global* effective channel vector decreases as the number of antennas used for a combining process increases [14, Lemma 3]. Second, the sum-rate grows like $M \log_2(\log K/2)$ because user candidates are reduced by half.

In this section, we develop an analytical framework weighing the pros and cons of the proposed cooperative feedback algorithm. Based on the analytical framework, an adaptive cooperation algorithm is proposed in order to activate/deactivate the proposed cooperation strategy according to channel and network conditions.

A. Loss in Local Channel Quantization

Before investigating the received signal of MU, we pause to analyze the channel quantization error induced in the process of *local* combining. As discussed in Section II-B, the channel quantization error between the normalized virtual channel vector $\frac{\mathbf{h}_{b|q}^{\text{virt}}}{\|\mathbf{h}_{b|q}^{\text{virt}}\|_2}$ and the target codeword \mathbf{d}^q is quantified by

$$S \doteq \sin^2 \phi_{b|q} = 1 - |(\mathbf{d}^q)^H \mathbf{h}_{b|q}^{\text{virt}} / \|\mathbf{h}_{b|q}^{\text{virt}}\|_2|^2, \quad (25)$$

where $\phi_{b|q}$ is the difference in angle defined in (12). It is verified in [14] that each error follows $\beta(M-N, N)$ random variable and its cumulative distribution function (cdf) can be approximated for small s , with $\delta = \binom{M-1}{N-1}^{\frac{-1}{M-N}}$, according to

$$F_S(s) \simeq \binom{M-1}{N-1} s^{M-N} \mathbb{1}_{[0,\delta]}(s) + \mathbb{1}_{(\delta,1]}(s). \quad (26)$$

The *local* CDI is obtained by selecting the codeword corresponding to the smallest quantization error from among Q^{cl} error terms $\sin^2 \phi_{b|q}$, $q \in \{1, \dots, Q^{\text{cl}}\}$. The channel quantization error corresponding to the *local* CDI can be studied by deriving the distribution of the smallest quantization error

$$\sin^2 \phi_b \doteq \sin^2 \phi_{b|\hat{q}},$$

where the index of the codeword in (13) is rewritten by

$$\hat{q} = \arg \min_{q \in \{1, \dots, Q^{\text{cl}}\}} \sin^2 \phi_{b|q}. \quad (27)$$

Based on the largest order statistics, we derive the expectation of the smallest quantization error in the following proposition.

Proposition 1: The expectation of the channel quantization error corresponding to the *local* CDI is approximated by

$$\mathbb{E}[\sin^2 \phi_b] \simeq Q^{\text{cl}} \binom{M-1}{N-1}^{\frac{-1}{M-N}} \mathbf{B} \left(Q^{\text{cl}}, \frac{M-N+1}{M-N} \right).$$

Proof: Minimizing the quantization error is the same as maximizing the normalized beamforming gain

$$C \doteq \cos^2 \phi_{b|q} = |(\mathbf{d}^q)^H \mathbf{h}_{b|q}^{\text{virt}} / \|\mathbf{h}_{b|q}^{\text{virt}}\|_2|^2$$

The cdf of the normalized beamforming gain is given by

$$\begin{aligned} F_C(c) &= 1 - F_S(1-c) \\ &\simeq 1 - \left(\binom{M-1}{N-1} (1-c)^{M-N} \mathbb{1}_{[0,\delta]}(1-c) + \mathbb{1}_{(\delta,1]}(1-c) \right) \\ &\stackrel{(a)}{=} 1 - \left(\binom{M-1}{N-1} (1-c)^{M-N} \mathbb{1}_{[1-\delta,1]}(c) + \mathbb{1}_{[0,1-\delta)}(c) \right) \\ &\stackrel{(b)}{=} \left(1 - \binom{M-1}{N-1} (1-c)^{M-N} \right) \mathbb{1}_{[1-\delta,1]}(c), \end{aligned}$$

where (a) is derived because $\mathbb{1}_{[0,\delta]}(1-c) = \mathbb{1}_{[1-\delta,1]}(c)$, $\mathbb{1}_{(\delta,1]}(1-c) = \mathbb{1}_{[0,1-\delta)}(c)$, and (b) is derived because $F_C(c) = 0$ when $0 \leq c < 1 - \delta$.

The normalized beamforming gain corresponding to the selected codeword (*local* CDI) is written as

$$G \doteq \cos^2 \phi_b = \max_{q \in \{1, \dots, Q^{\text{cl}}\}} \cos^2 \phi_{b|q}.$$

The probability that the largest beamforming gain is smaller than an arbitrary number g is defined according to $\Pr(\cos^2 \phi_b < g) = \prod_{q=1}^{Q^{\text{cl}}} \Pr(\cos^2 \phi_{b|q} < g)$. Therefore, the cdf of G is defined with the cdf of C such as

$$\begin{aligned} F_G(g) &\doteq (F_C(g))^{Q^{\text{cl}}} \\ &\simeq \left(1 - \binom{M-1}{N-1} (1-g)^{M-N} \right)^{Q^{\text{cl}}} \mathbb{1}_{[1-\delta,1]}(g). \end{aligned}$$

Because G is a non-negative random variable, the expectation of G can be derived such that

$$\begin{aligned} \mathbb{E}[G] &\simeq 1 - \int_0^1 F_G(g) dg \\ &= 1 - \sum_{q=0}^{Q^{\text{cl}}} \binom{Q^{\text{cl}}}{q} (-1)^q \binom{M-1}{N-1}^q \int_{1-\delta}^1 (1-g)^{q(M-N)} dg \end{aligned}$$

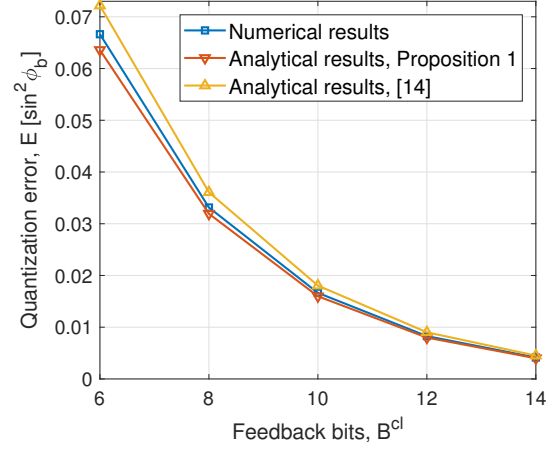


Fig. 3. Quantization error for QBC ($M = 4, N = 2$).

$$\begin{aligned} &= 1 - \delta \sum_{q=0}^{Q^{\text{cl}}} \frac{\binom{Q^{\text{cl}}}{q} (-1)^q}{q(M-N+1)} \\ &\stackrel{(a)}{=} 1 - \delta \sum_{q=0}^{Q^{\text{cl}}} \frac{(-Q^{\text{cl}})_q}{q! (q + \frac{1}{M-N})} \left(\frac{1}{M-N} \right) \\ &= 1 - \delta \frac{\Gamma(\frac{1}{M-N} + 1) Q^{\text{cl}} (Q^{\text{cl}} - 1)!}{\Gamma(\frac{1}{M-N} + Q^{\text{cl}} + 1)} \\ &= 1 - Q^{\text{cl}} \binom{M-1}{N-1}^{\frac{-1}{M-N}} \mathbf{B} \left(Q^{\text{cl}}, \frac{M-N+1}{M-N} \right), \end{aligned}$$

where (a) is derived based on [26, 6.6.8].

The expectation of the quantization error corresponding to the *local* CDI is approximated such that

$$\mathbb{E}[\sin^2 \phi_b] \simeq Q^{\text{cl}} \binom{M-1}{N-1}^{\frac{-1}{M-N}} \mathbf{B} \left(Q^{\text{cl}}, \frac{M-N+1}{M-N} \right),$$

because $\sin^2 \phi_b = 1 - \cos^2 \phi_b$. This completes the proof. ■

Finally, the accuracy of the quantization error in Proposition 1 and the formulation in [14], i.e., $[Q^{\text{cl}} \binom{M-1}{N-1}]^{\frac{-1}{M-N}}$, are evaluated by numerical results in Fig. 3. It is shown that our formulation in Proposition 1 shows better accuracy than the formulation in [14]. Further, we point out that the quantization error is better fitted to the numerical results as the feedback bits B^{cl} increase because the cdf in (26) is valid for small s .

B. Received Signal of MU

We take a closer look at the received signal of MU in (24). Assuming MU a is scheduled to use the m -th beamformer \mathbf{c}^m (meaning that $\bar{u}^m = a$), the received signal is written by

$$\begin{aligned} \bar{y}_{a|m} &= \sqrt{\rho} \bar{\mathbf{z}}_{a|m}^H \bar{\mathbf{H}}_a \left(\frac{[\mathbf{c}^1, \dots, \mathbf{c}^M]}{\sqrt{M}} \right) \mathbf{s} + \bar{\mathbf{z}}_{a|m}^H \bar{\mathbf{n}}_a \quad (28) \\ &= \sqrt{\frac{\rho}{M}} \left((\bar{\mathbf{h}}_{a|m}^{\text{eff}})^H \mathbf{c}^m s_m + \sum_{\ell=1, \ell \neq m}^M (\bar{\mathbf{h}}_{a|m}^{\text{eff}})^H \mathbf{c}^\ell s_\ell \right) + \bar{n}_{a|m}, \end{aligned}$$

where $\bar{\mathbf{h}}_{a|m}^{\text{eff}} \doteq \bar{\mathbf{H}}_a^H \bar{\mathbf{z}}_{a|m}$ is the *global* effective channel vector, and $\bar{n}_{a|m} \doteq \bar{\mathbf{z}}_{a|m}^H \bar{\mathbf{n}}_a \sim \mathcal{CN}(0, 1)$ is the combined noise. In

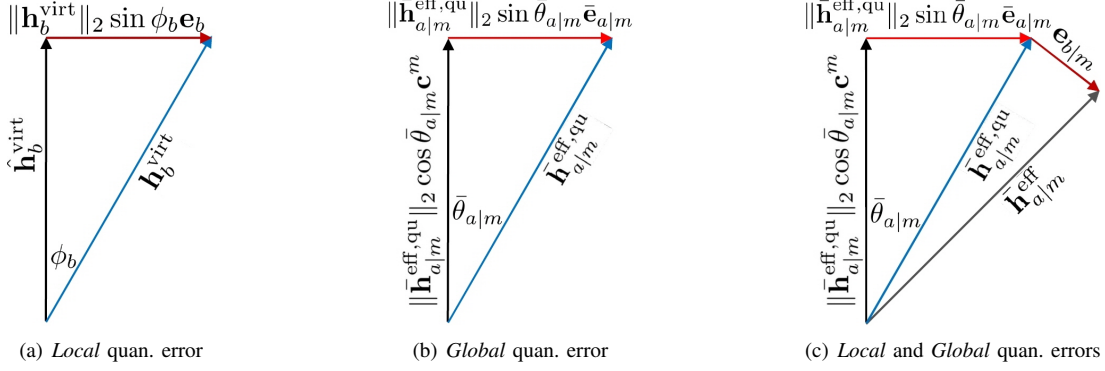


Fig. 4. Channel quantization errors in cooperative feedback algorithm.

$$y_{a|m} = \sqrt{\frac{\rho}{M}} \left(\underbrace{(\|\bar{\mathbf{h}}_{a|m}^{\text{eff,qu}}\|_2 \cos \bar{\theta}_{a|m} \mathbf{c}^m + \mathbf{e}_{b|m})^H \mathbf{c}^m}_{(I)} s_m + \sum_{\ell \neq m} \underbrace{\|\bar{\mathbf{h}}_{a|m}^{\text{eff,qu}}\|_2 \sin \bar{\theta}_{a|m} \bar{\mathbf{e}}_{a|m}^H \mathbf{c}^\ell}_{(II)} s_\ell + \sum_{\ell \neq m} \underbrace{\mathbf{e}_{b|m}^H \mathbf{c}^\ell}_{(III)} s_\ell \right) + \underbrace{\bar{n}_{a|m}}_{(IV)}. \quad (35)$$

order to examine *beamforming gain* and *interuser interference*, we must investigate the cross-correlations between the *global* effective channel vector $\bar{\mathbf{h}}_{a|m}^{\text{eff}}$ and codewords in \mathcal{C} .

The *global* effective channel vector is computed through two antenna combining processes (*locally* in AU and *globally* in MU) and each antenna combining process causes an individual quantization error. Before investigating both quantization errors jointly, we discuss each quantization error separately. First, we discuss the channel quantization error caused in the process of virtual vector quantization using *local* codebook \mathcal{D} . Note that the *local* quantization error is presented in Section III-1. As illustrated in Fig. 4(a), the virtual channel vector $\mathbf{h}_b^{\text{virt}}$ in (21) is divided into the quantized virtual channel vector $\hat{\mathbf{h}}_b^{\text{virt}}$ in (15) and the *local* error vector \mathbf{e}_b according to

$$\begin{aligned} \mathbf{h}_b^{\text{virt}} &= (\|\mathbf{h}_b^{\text{virt}}\|_2 \cos \phi_b) \mathbf{v}_b + (\|\mathbf{h}_b^{\text{virt}}\|_2 \sin \phi_b) \mathbf{e}_b \\ &= \hat{\mathbf{h}}_b^{\text{virt}} + (\|\mathbf{h}_b^{\text{virt}}\|_2 \sin \phi_b) \mathbf{e}_b, \end{aligned} \quad (29)$$

where $\sin^2 \phi_b = 1 - |\mathbf{v}_b^H \mathbf{h}_b^{\text{virt}} / \|\mathbf{h}_b^{\text{virt}}\|_2|^2$ quantifies the *local* quantization error. Second, we discuss the channel quantization error caused in the process of effective vector quantization using the *global* codebook \mathcal{C} . Note that the *global* quantization error is presented in Section III-2. As depicted in Fig. 4(b), the effective channel vector $\bar{\mathbf{h}}_{a|m}^{\text{eff,qu}}$ in (17) is divided into the target codeword \mathbf{c}^m and the *global* error vector $\bar{\mathbf{e}}_{a|m}$ such that

$$\bar{\mathbf{h}}_{a|m}^{\text{eff,qu}} = (\|\bar{\mathbf{h}}_{a|m}^{\text{eff,qu}}\|_2 \cos \bar{\theta}_{a|m}) \mathbf{c}^m + (\|\bar{\mathbf{h}}_{a|m}^{\text{eff,qu}}\|_2 \sin \bar{\theta}_{a|m}) \bar{\mathbf{e}}_{a|m}, \quad (30)$$

where $\sin^2 \bar{\theta}_{a|m} = 1 - |(\mathbf{c}^m)^H \bar{\mathbf{h}}_{a|m}^{\text{eff,qu}} / \|\bar{\mathbf{h}}_{a|m}^{\text{eff,qu}}\|_2|^2$ quantifies the *global* quantization error.

We now consider both quantization errors jointly. When MU conducts post-signal processing, the *global* combiner $\bar{\mathbf{z}}_{a|m}$ is used to combine spatial dimensions of the *global* channel matrix $\bar{\mathbf{H}}_a$ in (23) for downlink transmissions. We call $\bar{\mathbf{H}}_a$ the downlink channel matrix. It should be noted that the downlink channel matrix $\bar{\mathbf{H}}_a$ includes the *unquantized* virtual vector $\mathbf{h}_b^{\text{virt}}$ in (14). However, the *global* combiner is computed

using another *global* channel matrix $\bar{\mathbf{H}}_a^{\text{qu}}$ in (16) including the *quantized* virtual vector $\hat{\mathbf{h}}_b^{\text{virt}}$ in (15). The correspondence between the downlink channel matrix and the *global* channel matrix must be investigated because the combined quantization error occurs due to the difference between $\bar{\mathbf{H}}_a$ and $\bar{\mathbf{H}}_a^{\text{qu}}$.

First, we rewrite the downlink channel matrix in (23) by plugging the virtual channel vector in (29) according to

$$\begin{aligned} \bar{\mathbf{H}}_a &= \begin{bmatrix} \mathbf{H}_a \\ (\mathbf{h}_b^{\text{virt}})^H \end{bmatrix} \\ &= \begin{bmatrix} \mathbf{H}_a \\ (\hat{\mathbf{h}}_b^{\text{virt}})^H \end{bmatrix} + \begin{bmatrix} \mathbf{0}_{N,M} \\ (\|\mathbf{h}_b^{\text{virt}}\|_2 \sin \phi_b) \mathbf{e}_b^H \end{bmatrix} \\ &= \bar{\mathbf{H}}_a^{\text{qu}} + [\mathbf{0}_{M,N}, (\|\mathbf{h}_b^{\text{virt}}\|_2 \sin \phi_b) \mathbf{e}_b]^H. \end{aligned} \quad (31)$$

As depicted in Fig. 4(c), the effective channel vector in (28), corresponding to downlink transmissions, is written by⁹

$$\begin{aligned} \bar{\mathbf{h}}_{a|m}^{\text{eff}} &= \bar{\mathbf{H}}_a^H \bar{\mathbf{z}}_{a|m} \\ &= (\bar{\mathbf{H}}_a^{\text{qu}})^H \bar{\mathbf{z}}_{a|m} + [\mathbf{0}_{M,N}, (\|\mathbf{h}_b^{\text{virt}}\|_2 \sin \phi_b) \mathbf{e}_b] \bar{\mathbf{z}}_{a|m} \\ &= \bar{\mathbf{h}}_{a|m}^{\text{eff,qu}} + \mathbf{e}_{b|m}, \end{aligned} \quad (32)$$

where the effective channel vector $\bar{\mathbf{h}}_{a|m}^{\text{eff,qu}} = (\bar{\mathbf{H}}_a^{\text{qu}})^H \bar{\mathbf{z}}_{a|m}$ is defined in (17) and the error vector is given by

$$\mathbf{e}_{b|m} \doteq ([\bar{\mathbf{z}}_{a|m}]_{N+1} \|\mathbf{h}_b^{\text{virt}}\|_2 \sin \phi_b) \mathbf{e}_b \in \mathbb{C}^M. \quad (33)$$

Second, we rewrite the downlink channel vector $\bar{\mathbf{h}}_{a|m}^{\text{eff}}$ by plugging the effective channel vector $\bar{\mathbf{h}}_{a|m}^{\text{eff,qu}}$ in (30) such that

$$\begin{aligned} \bar{\mathbf{h}}_{a|m}^{\text{eff}} &= \underbrace{(\|\bar{\mathbf{h}}_{a|m}^{\text{eff,qu}}\|_2 \cos \bar{\theta}_{a|m}) \mathbf{c}^m}_{(a)} \\ &\quad + \underbrace{(\|\bar{\mathbf{h}}_{a|m}^{\text{eff,qu}}\|_2 \sin \bar{\theta}_{a|m}) \bar{\mathbf{e}}_{a|m}}_{(b)} + \underbrace{\mathbf{e}_{b|m}}_{(c)}, \end{aligned} \quad (34)$$

where $\|\bar{\mathbf{h}}_{a|m}^{\text{eff,qu}}\|_2^2 \cos^2 \bar{\theta}_{a|m}$ in (a) denotes the beamforming

⁹We call $\bar{\mathbf{h}}_{a|m}^{\text{eff}}$ the downlink channel vector.

$$\begin{aligned}
\text{SINR}_{a|m} &\geq \frac{\frac{\rho}{M} \|\bar{\mathbf{h}}_{a|m}^{\text{eff,qu}}\|_2^2 \cos^2 \bar{\theta}_{a|m}}{\mathbb{E}[|\bar{n}_{a|m}|^2] + \frac{\rho}{M} \|\bar{\mathbf{h}}_{a|m}^{\text{eff,qu}}\|_2^2 \sin^2 \bar{\theta}_{a|m} \sum_{\ell=1, \ell \neq m}^M \underbrace{|\bar{\mathbf{e}}_{a|m}^H \mathbf{c}^\ell|^2}_{(i)} + \frac{\rho}{M} |[\bar{\mathbf{z}}_{a|m}]_{N+1}|^2 \|\mathbf{h}_b^{\text{virt}}\|_2^2 \sin^2 \phi_b \sum_{\ell=1}^M \underbrace{|\mathbf{e}_b^H \mathbf{c}^\ell|^2}_{(ii)}} \\
&= \frac{\frac{\rho}{M} \|\bar{\mathbf{h}}_{a|m}^{\text{eff,qu}}\|_2^2 \cos^2 \bar{\theta}_{a|m}}{1 + \frac{\rho}{M} \|\bar{\mathbf{h}}_{a|m}^{\text{eff,qu}}\|_2^2 \sin^2 \bar{\theta}_{a|m} + \frac{\rho}{M} |[\bar{\mathbf{z}}_{a|m}]_{N+1}|^2 \|\mathbf{h}_b^{\text{virt}}\|_2^2 \sin^2 \phi_b \sum_{\ell=1}^M |\mathbf{e}_b^H \mathbf{c}^\ell|^2} \\
&= \frac{\frac{\rho}{M} \|\bar{\mathbf{h}}_{a|m}^{\text{eff,qu}}\|_2^2 \cos^2 \bar{\theta}_{a|m}}{1 + \underbrace{\frac{\rho}{M} \|\bar{\mathbf{h}}_{a|m}^{\text{eff,qu}}\|_2^2 \sin^2 \bar{\theta}_{a|m}}_{(II)} + \underbrace{\frac{\rho}{M} |[\bar{\mathbf{z}}_{a|m}]_{N+1}|^2 \|\mathbf{h}_b^{\text{virt}}\|_2^2 \sin^2 \phi_b}_{(III)}}. \tag{36}
\end{aligned}$$

gain for data transmissions, (b) denotes the *global* quantization error, and (c) denotes the *local* quantization error. The relationship between the codeword \mathbf{c}^m and the *global* effective vector $\bar{\mathbf{h}}_{a|m}^{\text{eff}}$ is summarized in Fig. 4(c).

Finally, we rewrite the received signal of MU by plugging the downlink vector $\bar{\mathbf{h}}_{a|m}^{\text{eff}}$ in (34) into the input-output expression in (28). As presented in (35), the desired signal (I), *global* (interuser) interferences (II), *local* (interuser) interferences (III), and noise (IV) are clearly distinguished.

C. Analysis of signal-to-interference-plus-noise ratio

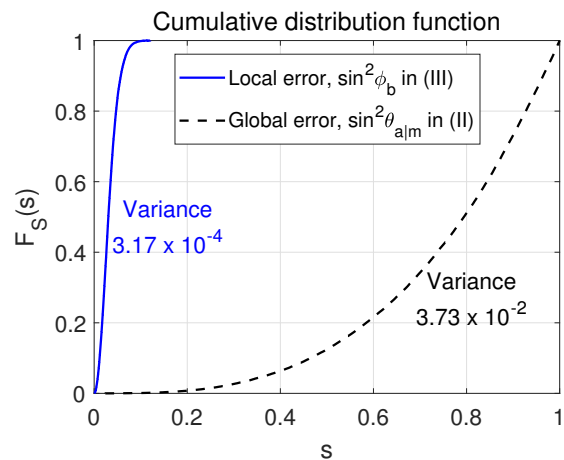
We analyze the SINR for all MUs in the network. Similar to [13], the lower bound of SINR is defined in (36) because $\sum_{\ell=1, \ell \neq m}^M |\mathbf{e}_b^H \mathbf{c}^\ell|^2 = \sum_{\ell=1}^M |\mathbf{e}_b^H \mathbf{c}^\ell|^2$ based on the assumption that the *local* quantization error $\mathbf{e}_{b|m}$ is orthogonal to the target codeword \mathbf{c}^m . We noted that the error vector $\mathbf{e}_{b|m}$ is replaced by (33) in order to show all the *local* interference terms clearly. To verify the second equality, we should recall that the unit-norm error vector $\bar{\mathbf{e}}_{a|m}$ is orthogonal to the target codeword \mathbf{c}^m . Since we consider a single unitary matrix for constructing the *global* codebook,¹⁰ the error vector is on the hyperplane, which is made up of $M - 1$ orthonormal codewords that are orthogonal to \mathbf{c}^m . The error vector is thus written as a linear combination of the orthonormal codewords as $\bar{\mathbf{e}}_{a|m} = \sum_{\ell=1, \ell \neq m}^M ((\mathbf{c}^\ell)^H \bar{\mathbf{e}}_{a|m}) \mathbf{c}^\ell$. The sum of terms in (i) is computed according to $\|\bar{\mathbf{e}}_{a|m}\|_2^2 = \sum_{\ell=1, \ell \neq m}^M |\bar{\mathbf{e}}_{a|m}^H \mathbf{c}^\ell|^2 = 1$, because \mathbf{c}^ℓ and $\bar{\mathbf{e}}_{a|m}$ are unit-norm vectors. The third equality follows because the sum of terms in (ii) is computed as

$$\sum_{\ell=1}^M |\mathbf{e}_b^H \mathbf{c}^\ell|^2 = \mathbf{e}_b^H (\mathbf{C}\mathbf{C}^H) \mathbf{e}_b = \|\mathbf{e}_b\|_2^2 = 1,$$

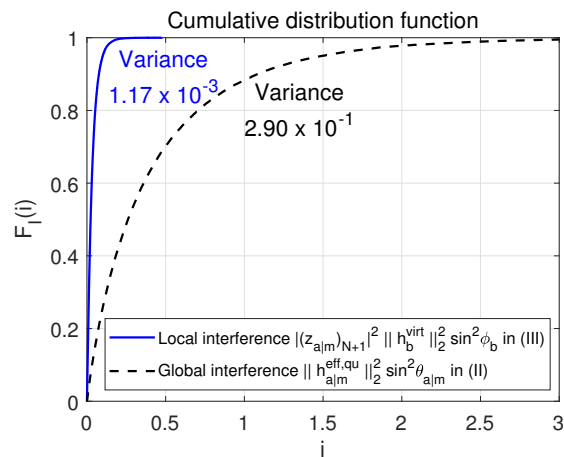
because $\mathbf{C} \doteq [\mathbf{c}^1, \dots, \mathbf{c}^M] \in \mathbb{C}^{M \times M}$ is the unitary matrix.

Unfortunately, it is not easy to derive the joint distribution between the *local* and *global* error terms in (36). For easy of analysis, we point out the fact that the size of the *local* codebook is much bigger than that of the *global* codebook such as $B^{\text{cl}} \gg B$. Moreover, $\sin^2 \phi_b$ is the minimum error selected among Q^{cl} *local* error terms, while $\cos^2 \bar{\theta}_{a|m}$ is an general *global* error term. For these reasons, the variance and

¹⁰If *global* codebook consists of more than M codewords, $|\bar{\mathbf{e}}_{a|m}^H \mathbf{c}^\ell|^2$ can be modeled by $\beta(1, M - 2)$ because $\bar{\mathbf{e}}_{a|m}$ and \mathbf{c}^ℓ independent and isotropically distributed on the $M - 1$ dimensional hyperplane orthogonal to \mathbf{c}^m [12].



(a) Distributions of *local* and *global* quan. errors



(b) Distributions of *local* and *global* interferences

Fig. 5. CDF of *local* and *global* variables ($M = 4$, $N = 2$, $B^{\text{cl}} = 8$).

magnitude of the *local* quantization error are smaller than those of the *global* quantization error, as shown in Fig. 5(a). It is also verified in Fig. 5(b) that the variance and magnitude of the *local* interference are small compared to those of the *global* interference. From these observations, we infer that the *local* interferences would have minimal effect on the SINR.

In this paper, we approximate the SINR by computing the expectation of *local* interference using similar logic that the

$$\text{SINR}_{a|m} \simeq \frac{\frac{\rho}{M} \|\bar{\mathbf{h}}_{a|m}^{\text{eff,qu}}\|_2^2 \cos^2 \bar{\theta}_{a|m}}{1 + \frac{\rho}{M} \|\bar{\mathbf{h}}_{a|m}^{\text{eff,qu}}\|_2^2 \sin^2 \bar{\theta}_{a|m} + \frac{\rho}{M} \mathbb{E}[|\bar{\mathbf{z}}_{a|m}|_{N+1}|^2] \|\mathbf{h}_b^{\text{virt}}\|_2^2 \sin^2 \phi_b}}{\frac{\rho}{M\alpha} \|\bar{\mathbf{h}}_{a|m}^{\text{eff,qu}}\|_2^2 \cos^2 \bar{\theta}_{a|m}} \doteq \bar{\gamma}_{a|m}. \quad (37)$$

$$\bar{\gamma}_{a|m} \simeq \frac{\rho \varrho^2}{M\alpha} \left(\log \left(\frac{\binom{M-1}{N} \bar{Q}^m}{\left(\frac{\rho \varrho^2}{M\alpha}\right)^{M-(N+1)}} \right) - (M - (N + 1)) \log \left(\log \left(\frac{\binom{M-1}{N} \bar{Q}^m}{\left(\frac{\rho \varrho^2}{M\alpha}\right)^{M-(N+1)}} \right) + \left(\frac{\rho \varrho^2}{M\alpha}\right)^{-1} \right) \right). \quad (39)$$

$$\gamma_{a|m} \simeq \frac{\rho}{M} \left(\log \left(\frac{\binom{M-1}{N-1} Q^m}{\left(\frac{\rho}{M}\right)^{M-N}} \right) - (M - N) \log \left(\log \left(\frac{\binom{M-1}{N-1} Q^m}{\left(\frac{\rho}{M}\right)^{M-N}} \right) + \left(\frac{\rho}{M}\right)^{-1} \right) \right). \quad (41)$$

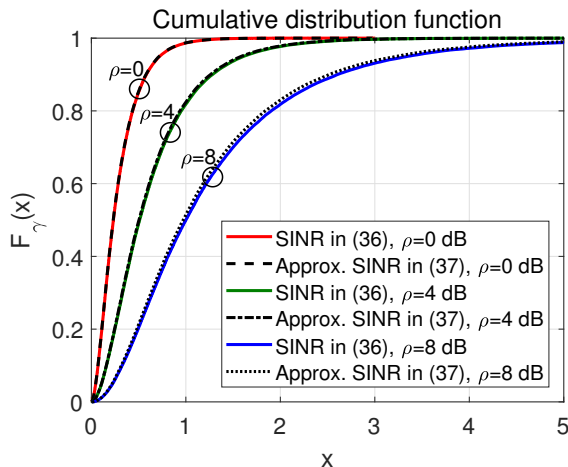


Fig. 6. CDF of SINR and approximated SINR ($M = 4$, $N = 2$, $B^{\text{cl}} = 8$).

absolute square of the noise term is commonly replaced by its expectation value when defining the SINR. We noted that the accuracy of this approximation is evaluated in the following paragraph. The expectation of *local* interference is

$$\begin{aligned} \mathbb{E}[|\bar{\mathbf{z}}_{a|m}|_{N+1}|^2 \|\mathbf{h}_b^{\text{virt}}\|_2^2 \sin^2 \phi_b] &\stackrel{(a)}{=} \frac{\mathbb{E}[\|\mathbf{h}_b^{\text{virt}}\|_2^2] \mathbb{E}[\sin^2 \phi_b]}{N+1} \\ &\stackrel{(b)}{=} \frac{(M-N+1) \mathbb{E}[\sin^2 \phi_b]}{N+1} \\ &\stackrel{(c)}{\simeq} \frac{(M-N+1)\omega}{N+1} \doteq \nu, \end{aligned}$$

because $|\bar{\mathbf{z}}_{a|m}|_{N+1}|^2$, $\|\mathbf{h}_b^{\text{virt}}\|_2^2$, and $\sin^2 \phi_b$ are independent. Note that (a) is derived because the absolute square of each entry of the *global* combiner $\bar{\mathbf{z}}_{a|m} \in \mathbb{C}^{N+1}$ is expected to be one over the number of entries, (b) is derived because the quantity $\|\mathbf{h}_b^{\text{virt}}\|_2^2$ of effective channel follows Chi-squared distribution $\chi_{2(M-N+1)}^2$ and its expectation is $M - N + 1$ [14, Lemma 3], and (c) is derived in Proposition 1, where the expectation of the quantization error is $\omega = Q^{\text{cl}} \binom{M-1}{N-1}^{\frac{-1}{M-N}} \mathbf{B}(Q^{\text{cl}}, \frac{M-N+1}{M-N})$. The SINR is approximated in (37), where $\alpha \doteq 1 + \rho\nu/M$ denotes the noise-plus-*local* interference for a given SNR ρ .

We evaluate the accuracy of our approximation by comparing the cdf of the approximated SINR in (37) with that of the SINR in (36). As shown in Fig. 6, the SINR is well approximated by (37) in three different SNR scenarios. We thus conclude that the operation of replacing the *local* interference by its

expectation value would lead a minimal effect on the SINR. For easy of analysis, we use the approximated SINR for the rest of sections.

Further, the distribution of the quantity $\|\bar{\mathbf{h}}_{a|m}^{\text{eff,qu}}\|_2^2$ in (37) is derived in the following proposition.

Proposition 2: The squared norm of *global* effective vector

$$\mathbf{U} \doteq \|\bar{\mathbf{h}}_{a|m}^{\text{eff,qu}}\|_2^2 = \|(\bar{\mathbf{H}}_a^{\text{qu}})^H \bar{\mathbf{z}}_{a|m}\|_2^2$$

follows Chi-squared distribution $\chi_{2(M-N)}^2$ and its pdf is $f_{\mathbf{U}}(u) \simeq \frac{u^{M-N-1} e^{-u/\varrho^2}}{\varrho^{2(M-N)} \Gamma(M-N)}$ with the variance $\varrho^{-2} \doteq \frac{1}{N+1} [N + \frac{M}{(1-\omega)(M-N+1)}]$ and $\omega \doteq Q^{\text{cl}} \binom{M-1}{N-1}^{\frac{-1}{M-N}} \mathbf{B}(Q^{\text{cl}}, \frac{M-N+1}{M-N})$.

Proof: For the proof, see Appendix A. ■

Finally, the cdf of approximated SINR $X \doteq \bar{\gamma}_{a|m}$ in (37) is derived based on the pdf of $\|\bar{\mathbf{h}}_{a|m}^{\text{eff,qu}}\|_2^2$ according to

$$F_X(x) \simeq 1 - \frac{\binom{M-1}{N} e^{-\frac{M\alpha}{\rho\varrho^2}x}}{(x+1)^{M-N-1}}. \quad (38)$$

Proof: For the proof, see [13] and [22, Lemma 3]. ■

D. Cooperation Mode Switching Algorithm

We develop a cooperation mode switching algorithm based on the expectation of a sum-rate. To estimate sum-rate throughput, we derive the cdf of the SINR for the scheduled MUs in $\bar{\mathcal{U}}$. By using a similar logic from [22, Theorem 1], the SINR for the m -th selected MU is estimated as in (39) with the cdf of SINR in (38). We now take a closer look at \bar{Q}^m meaning the number of CQI candidates for the m -th user selection process. Since each user generates M CQIs, the total number of CQI candidates is given by KM . Because the user having the largest CQI is selected from the remaining CQI candidates, the scheduled user and the codeword is excluded for the following user selection process. The number of CQI candidates in the m -th user selection process is defined by

$$\bar{Q}^m \doteq (K - 2(m - 1))(M - (m - 1)).$$

Finally, the sum-rate of the multiuser MIMO system relying upon the proposed cooperative feedback is estimated as

$$R_{\text{prop}} \simeq \sum_{m=1}^M \log_2 (1 + \bar{\gamma}_{a|m}) \quad (40)$$

with the estimated SINR for the scheduled MUs in (39).

Remark 1: When the cooperative feedback is not activated, the sum-rate of the multiuser MIMO system is estimated in [22] according to $R_{\text{conv}} \simeq \sum_{m=1}^M \log_2(1 + \gamma_{|m})$. The SINR for the scheduled user is defined in (41) and the number of CQI candidates is given by $Q^m \doteq (K - (m - 1))(M - (m - 1))$.

In the proposed cooperation mode switching algorithm, multiuser MIMO systems activate the cooperative feedback mode when the differential sum-rate is positive such that

$$\Delta R \doteq R_{\text{prop}} - R_{\text{conv}} > 0. \quad (42)$$

V. NUMERICAL RESULTS

In this section, we evaluate the performance of the cooperative feedback algorithm based on the sum-rate defined as

$$R_{\text{num}} \doteq \sum_{m=1}^M \log_2(1 + \tilde{\gamma}_{|m}),$$

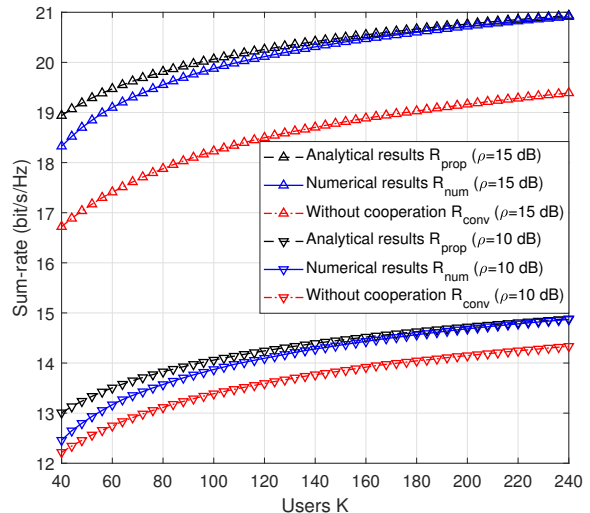
where the SINR for the m -th scheduled user is computed numerically according to

$$\tilde{\gamma}_{|m} \doteq \frac{|(\bar{\mathbf{h}}_{\bar{u}^m}^{\text{eff}})^H \mathbf{c}^m|^2}{\frac{M}{\rho} + \sum_{\ell=1, \ell \neq m}^M |(\bar{\mathbf{h}}_{\bar{u}^m}^{\text{eff}})^H \mathbf{c}^\ell|^2}.$$

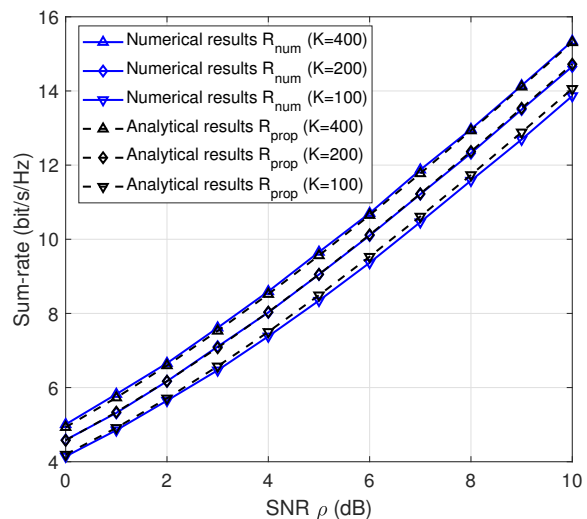
Note that \bar{u}^m denotes the scheduled MU exploiting the m -th codeword \mathbf{c}^m . The sum-rate performance is evaluated numerically from Monte-carlo simulations with 10,000 independent channels (solid blue lines in Fig. 7). Moreover, the sum-rate performance is verified analytically with the formulation derived in Section IV-D (dotted black lines in Fig. 7).

We first investigate the accuracy of the sum-rate formulation R_{prop} derived in (40). In Fig. 7(a), we compare the numerical results and the sum-rate formulation against the number of users K . In Figs. 7(b) and 7(c), the numerical results and the sum-rate formulation are compared for a variety of user numbers (between 50 and 400) against SNR ρ . The accuracy of the sum-rate formulation is verified by assuming the cooperation mode is activated. It should be noted that the sum-rate formulation is derived in Section IV-D based on the largest order statistics [27]. According to the extreme value theory, the differences between the numerical results and the sum-rate in (40) decrease as the number of users K increases. In Figs. 7, it is shown that the differences between the numerical results and the sum-rate formulation are negligible, especially when there are a large number of users on the MTC network. Moreover, the error term ν in (37) is matched to the numerical results when the overhead for the cooperation link B^{cl} is large. It is expected that the sum-rate formulation will be better fitted to the numerical results as the size of the *local* codebook B^{cl} increases.

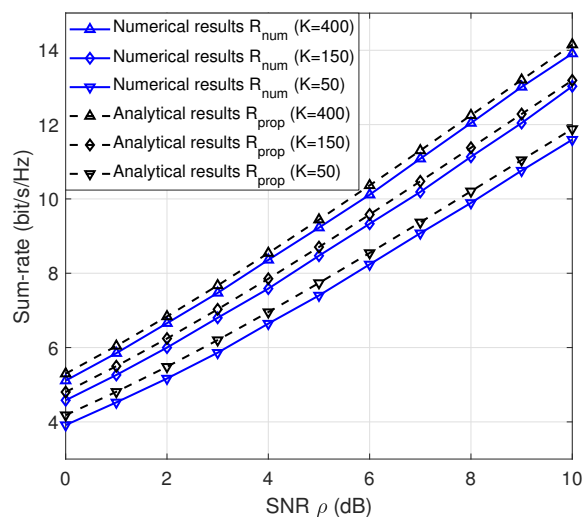
In Figs. 8(a) and 8(b), we evaluate the sum-rate performances of the cooperation mode switching algorithm. The proposed algorithm shows better sum-rate estimation performance when the number of users is sufficiently large because the cooperation mode switching algorithm is developed based on the extreme value theory [27]. In Fig. 8(c), we take a closer look at the cross point between the cooperative feedback activation mode and the cooperative feedback deactivation mode ($M = 4$, $N = 3$, $B^{\text{cl}} = 6$). The estimated mode switching point (square) and the mode switching point in the numerical results (circle) are



(a) $M = 4$, $N = 3$, $B^{\text{cl}} = 4$

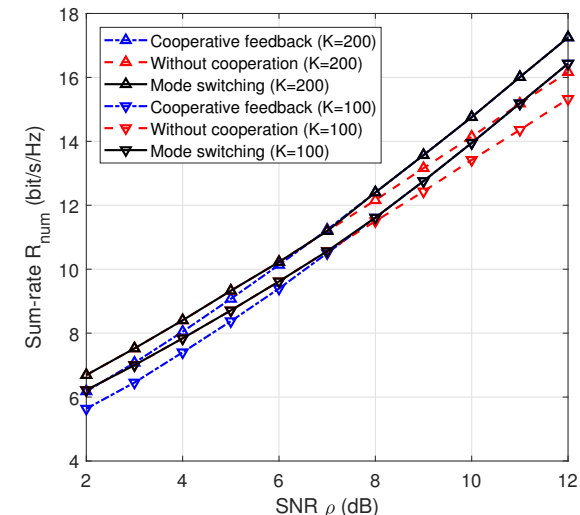
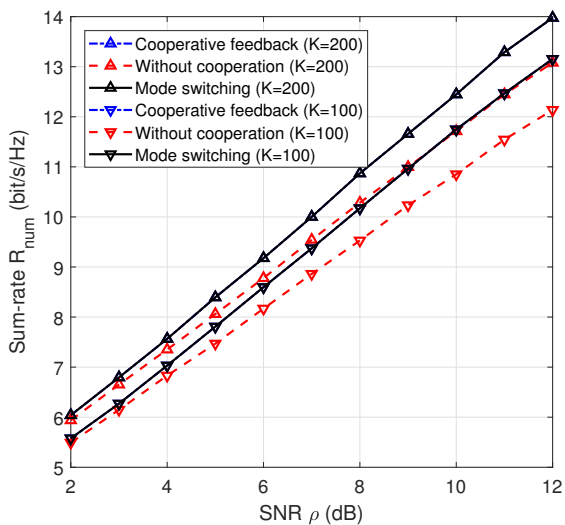
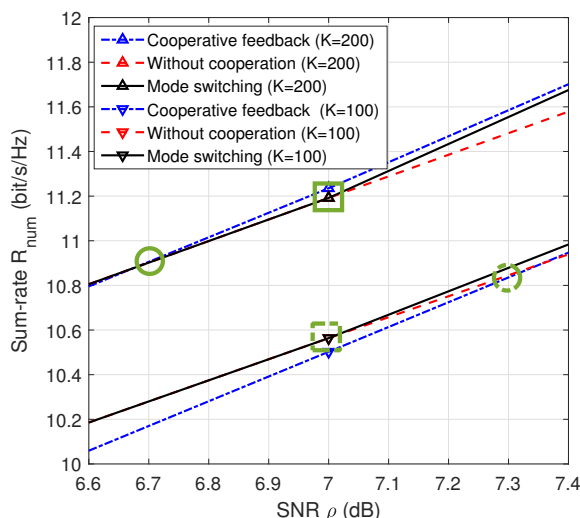


(b) $M = 4$, $N = 3$, $B^{\text{cl}} = 4$



(c) $M = 4$, $N = 2$, $B^{\text{cl}} = 8$

Fig. 7. Comparison between numerical and analytical results.

(a) $M = 4, N = 3, B^{cl} = 6$ (b) $M = 4, N = 2, B^{cl} = 4$ 

(c) Mode switching points in Fig. 8(a)

Fig. 8. Sum-rate performance of adaptive cooperation algorithm.

both within the range of a 0.3-dB window. This result means that the proposed adaptive cooperation algorithm finds mode switching points well based on the given information of SNR ρ and system parameters, i.e., K , B^{cl} , M , and N . In Fig. 8(b), the mode switching algorithm always triggers cooperation mode. For this reason, the cooperative feedback algorithm (blue line) and mode switching algorithm (black line) produce the same numerical results and the numerical results overlap. Numerical simulations verify that the cooperative feedback algorithms outperform conventional multiuser MIMO systems that do not exploit cooperative feedback mode.

VI. CONCLUSION

In this paper, we developed limited feedback frameworks suitable for multiuser systems in MTC networks. First, we proposed the user cooperation-based limited feedback strategy to obtain high-resolution CSI with minimal additional burden on the current FDD-based communication architecture. We focused on reducing channel quantization errors by allowing a limited amount of CSI exchange between close-in users. In the proposed algorithm, some multiuser resources are used to enhance channel quantization performance while minimizing multiuser diversity gain degradation that this approach entails. Second, we carried out sum-rate throughput analysis to solve the trade-off problem between channel quantization performance and multiuser diversity gain. Based on the analytical studies, we developed the cooperation mode switching algorithm in order to activate/deactivate cooperation mode according to channel and network conditions without transmitter interventions. Numerical results verified that the proposed algorithm improves sum-rate throughput because the multiuser resources are used to obtain high-resolution CSI.

APPENDIX A

NORM OF THE GLOBAL EFFECTIVE CHANNEL VECTOR

We study statistical properties of the *global* channel matrix $\bar{\mathbf{H}}_a^{qu} = [\mathbf{H}_a^H, \hat{\mathbf{h}}_b^{virt}]^H$ in (16) to analyze the quantity

$$U \doteq \|\bar{\mathbf{h}}_{a|m}^{eff,qu}\|_2^2 = \|(\bar{\mathbf{H}}_a^{qu})^H \bar{\mathbf{z}}_{a|m}\|_2^2 \quad (43)$$

of the *global* effective channel vector. The *global* channel matrix is composed of \mathbf{H}_a including N channel vectors of MU and the (quantized) virtual channel vector $\hat{\mathbf{h}}_b^{virt}$ transferred from AU. It is already known that the entries in \mathbf{H}_a follow $\mathcal{CN}(0, 1)$. We focus on analyzing the virtual channel in (15),

$$\begin{aligned} \hat{\mathbf{h}}_b^{virt} &= \cos \phi_b \|\mathbf{h}_b^{virt}\|_2 \mathbf{v}_b \\ &\doteq \cos \phi_b \mathbf{v}_b^{virt} \in \mathbb{C}^M, \end{aligned}$$

where we define $\mathbf{v}_b^{virt} \doteq \|\mathbf{h}_b^{virt}\|_2 \mathbf{v}_b$. Notice that $\cos \phi_b$, $\|\mathbf{h}_b^{virt}\|_2$, and \mathbf{v}_b are independent. Since \mathbf{v}_b is a unit-norm vector with isotropically distributed entries, the quantity $A \doteq \|\mathbf{v}_b^{virt}\|_2^2 = \|\mathbf{h}_b^{virt}\|_2^2$ follows Chi-squared distribution $\chi_{2(M-N+1)}^2$, where its pdf is given by

$$f_A(a) = \frac{a^{M-N} e^{-a/(2\sigma_a^2)}}{(2\sigma_a^2)^{(M-N+1)} \Gamma(M-N+1)}$$

with the variance $\sigma_a^2 = \frac{1}{2}$ [28], [29].

All other entries in the *global* channel matrix $\bar{\mathbf{H}}_a^{\text{qu}}$ follow Gaussian distribution so that it would be good in analyzing the quantity $\|\bar{\mathbf{h}}_{a|m}^{\text{eff,qu}}\|_2^2$ if the entries in $\mathbf{v}_b^{\text{virt}}$ also follow Gaussian distribution. However, the quantity $\|\mathbf{v}_b^{\text{virt}}\|_2^2$ has the distribution of the $(M - N + 1)$ -dimensional vector, while the vector is in the M -dimensional complex space. For this reason, $\mathbf{v}_b^{\text{virt}}$ cannot be modeled by Gaussian random variable although its phase follows uniform distribution in the interval $[0, 2\pi)$ and the quantity $\|\mathbf{v}_b^{\text{virt}}\|_2^2$ follows Chi-squared distribution. For easy of analysis, we made two assumptions as follows¹¹:

- First, we assume that the quantity $\|\mathbf{v}_b^{\text{virt}}\|_2^2$ can be approximated by $B \doteq \|\check{\mathbf{v}}_b^{\text{virt}}\|_2^2$ that follows Chi-squared distribution¹² χ_{2M}^2 with M degree of freedom (DoF), where its pdf is given by $f_B(b) = \frac{b^{M-1} e^{-b/(2\sigma_b^2)}}{(2\sigma_b^2)^M \Gamma(M)}$ with the variance $\sigma_b^2 = \frac{M-N+1}{2M}$. The approximation is the result of changing DoF while adjusting its variance to make $E[B]$ equal to $E[A]$ such that

$$\begin{aligned} E[B] &= \int_0^\infty b f_B(b) db = \frac{\int_0^\infty b^M e^{-b/(2\sigma_b^2)} db}{(2\sigma_b^2)^M \Gamma(M)} \\ &= \frac{(2\sigma_b^2)^{M+1} \Gamma(M+1)}{(2\sigma_b^2)^M \Gamma(M)} = M - N + 1. \end{aligned}$$

- Second, we assume that the random variable $\cos^2 \phi_b$ can be replaced by its expectation value $E[\cos^2 \phi_b] = 1 - \omega$ by using similar method¹³ in Section IV-C. The expectation of the quantization error is derived in Proposition 1 such that $\omega = Q^{\text{cl}} \binom{M-1}{N-1}^{\frac{-1}{M-N}} \mathbf{B}(Q^{\text{cl}}, \frac{M-N+1}{M-N})$.

As a result of the above assumptions, the virtual vector can be approximated by $\check{\mathbf{h}}_b^{\text{virt}} \simeq \check{\mathbf{h}}_b^{\text{virt}}$, where its entries follow $\mathcal{CN}(0, \frac{(1-\omega)(M-N+1)}{M})$. After all the discussions of the entries in $\bar{\mathbf{H}}_a^{\text{qu}}$, the *global* channel matrix is modeled by

$$\bar{\mathbf{H}}_a^{\text{qu}} \simeq \mathbf{R}^{\frac{1}{2}} \bar{\mathbf{H}}_a^{\text{w}} \doteq \check{\mathbf{H}}_a^{\text{qu}} \quad (44)$$

where $\bar{\mathbf{H}}_a^{\text{w}}$ is the *global* channel matrix having entries that follow $\mathcal{CN}(0, 1)$, and the covariance matrix is given by

$$\mathbf{R} \doteq \begin{bmatrix} \mathbf{I}_N & \mathbf{0}_{N,1} \\ \mathbf{0}_{1,N} & \frac{(1-\omega)(M-N+1)}{M} \end{bmatrix} \in \mathbb{C}^{(N+1) \times (N+1)}. \quad (45)$$

The squared norm of the *global* effective channel vector is now approximated by

$$\|\bar{\mathbf{h}}_{a|m}^{\text{eff,qu}}\|_2^2 \simeq \frac{\|(\check{\mathbf{H}}_a^{\text{qu}})^H \bar{\mathbf{u}}_{a|m}\|_2^2}{\|\bar{\mathbf{u}}_{a|m}\|_2^2} = \|\bar{\mathbf{u}}_{a|m}\|_2^{-2} \doteq D, \quad (46)$$

because $(\check{\mathbf{H}}_a^{\text{qu}})^H \bar{\mathbf{u}}_{a|m} = \mathbf{c}^{\text{proj},m}$, as shown in (5) and (6). We derive the distribution of $\|\bar{\mathbf{u}}_{a|m}\|_2^{-2}$.

Proposition 3: The distribution of $\|\bar{\mathbf{u}}_{a|m}\|_2^{-2}$ is the same as the distribution of $\frac{\mathbf{w}^H \mathbf{w}}{\mathbf{w}^H [\check{\mathbf{H}}_a^{\text{qu}} (\check{\mathbf{H}}_a^{\text{qu}})^H]^{-1} \mathbf{w}}$, where $\mathbf{w} \in \mathcal{W}$ is the

column vector that is subject to

$$\mathcal{W} \doteq \left\{ \mathbf{w} \in \mathbb{C}^{N+1} : [\mathbf{w}]_n = \frac{e^{j\psi_n}}{\sqrt{N+1}}, \psi_n \sim \text{U}(0, 2\pi) \right\}.$$

Proof: For a given channel matrix $\check{\mathbf{H}}_a^{\text{qu}} \in \mathbb{C}^{(N+1) \times M}$, the covariance matrix of $\bar{\mathbf{u}}_{a|m}$ is computed according to

$$\begin{aligned} \mathbf{Z} &\doteq [(\check{\mathbf{H}}_a^{\text{qu}})^H]^\dagger E[\mathbf{c}^{\text{proj},m} (\mathbf{c}^{\text{proj},m})^H] [(\check{\mathbf{H}}_a^{\text{qu}})^H]^\dagger \\ &\stackrel{(a)}{=} \frac{[(\check{\mathbf{H}}_a^{\text{qu}} (\check{\mathbf{H}}_a^{\text{qu}})^H)^{-1} \check{\mathbf{H}}_a^{\text{qu}} (\check{\mathbf{H}}_a^{\text{qu}})^H (\check{\mathbf{H}}_a^{\text{qu}} (\check{\mathbf{H}}_a^{\text{qu}})^H)^{-1}]}{M} \\ &= \frac{[\check{\mathbf{H}}_a^{\text{qu}} (\check{\mathbf{H}}_a^{\text{qu}})^H]^{-1}}{M} = \left(\frac{[\check{\mathbf{H}}_a^{\text{qu}} (\check{\mathbf{H}}_a^{\text{qu}})^H]^{-\frac{1}{2}}}{\sqrt{M}} \right)^2, \end{aligned}$$

where (a) is derived with $E[\mathbf{c}^{\text{proj},m} (\mathbf{c}^{\text{proj},m})^H] = \frac{\mathbf{I}_M}{M}$ because $\mathbf{c}^{\text{proj},m}$ is an independent (unit-norm) vector that is isotropically distributed in \mathbb{C}^M . To study statistical distributions of the quantity $\|\bar{\mathbf{h}}_{a|m}^{\text{eff,qu}}\|_2^2$, we model the receive combiner as

$$\mathbf{u} \doteq \mathbf{Z}^{\frac{1}{2}} \mathbf{w}, \quad (47)$$

where $\mathbf{w} \in \mathcal{W}$ is the isotropically distributed column vector. By plugging the receive combiner in (47) into (46), the approximated norm square of the *global* effective channel vector is rewritten by

$$\begin{aligned} D &\doteq \frac{\|(\check{\mathbf{H}}_a^{\text{qu}})^H \mathbf{u}\|_2^2}{\|\mathbf{u}\|_2^2} = \frac{\mathbf{w}^H (\mathbf{Z}^{\frac{1}{2}} \check{\mathbf{H}}_a^{\text{qu}} (\check{\mathbf{H}}_a^{\text{qu}})^H \mathbf{Z}^{\frac{1}{2}}) \mathbf{w}}{\mathbf{w}^H (\mathbf{Z}^{\frac{1}{2}} \mathbf{Z}^{\frac{1}{2}}) \mathbf{w}} \\ &= \frac{\mathbf{w}^H ([\check{\mathbf{H}}_a^{\text{qu}} (\check{\mathbf{H}}_a^{\text{qu}})^H]^{-\frac{1}{2}} \check{\mathbf{H}}_a^{\text{qu}} (\check{\mathbf{H}}_a^{\text{qu}})^H [\check{\mathbf{H}}_a^{\text{qu}} (\check{\mathbf{H}}_a^{\text{qu}})^H]^{-\frac{1}{2}}) \mathbf{w}}{\mathbf{w}^H [\check{\mathbf{H}}_a^{\text{qu}} (\check{\mathbf{H}}_a^{\text{qu}})^H]^{-1} \mathbf{w}} \\ &= \frac{\mathbf{w}^H \mathbf{w}}{\mathbf{w}^H [\check{\mathbf{H}}_a^{\text{qu}} (\check{\mathbf{H}}_a^{\text{qu}})^H]^{-1} \mathbf{w}} \end{aligned}$$

and this completes the proof. \blacksquare

We note that $\check{\mathbf{H}}_a^{\text{qu}} (\check{\mathbf{H}}_a^{\text{qu}})^H \in \mathbb{C}^{(N+1) \times (N+1)}$ is the complex Wishart matrix with the covariance matrix \mathbf{R} in (45) and M DoF [28]. Based on [30, Theorem 3.2.12], we can derive that

$$\mathbf{W} \doteq \frac{\mathbf{w}^H \mathbf{R}^{-1} \mathbf{w}}{\mathbf{w}^H [\check{\mathbf{H}}_a^{\text{qu}} (\check{\mathbf{H}}_a^{\text{qu}})^H]^{-1} \mathbf{w}} = \frac{\varrho^{-2} \mathbf{w}^H \mathbf{w}}{\mathbf{w}^H (\check{\mathbf{H}}_a^{\text{qu}} (\check{\mathbf{H}}_a^{\text{qu}})^H)^{-1} \mathbf{w}}$$

follows Chi-squared distribution $\chi_{2(M-N)}^2$, where its pdf is given by $f_W(w) = \frac{w^{M-N-1} e^{-w/(2\sigma_w^2)}}{(2\sigma_w^2)^{M-N} \Gamma(M-N)}$ with the variance $\sigma_w^2 = \frac{1}{2}$ [28], [29]. Note that the numerator is rewritten by

$$\varrho^{-2} \doteq \frac{\text{Tr}(\mathbf{R}^{-1})}{N+1} = \frac{1}{N+1} \left[N + \frac{M}{(1-\omega)(M-N+1)} \right].$$

The random variable $D = \|\bar{\mathbf{u}}_{a|m}\|_2^{-2}$ in (46) is rewritten by

$$D = \varrho^2 \mathbf{W} = \sum_{\ell=1}^{2(M-N)} D_\ell^2, \quad (48)$$

where D_ℓ are the i.i.d. entries that follow Gaussian random variables with zero mean and variance $\frac{\varrho^2}{2}$. From these observations, the pdf of the quantity $U \sim \chi_{2(M-N)}^2$ of the *global* effective channel vector can be approximated by

$$f_U(u) \simeq \frac{u^{M-N-1} e^{-u/(2(\varrho^2/2))}}{(2(\varrho^2/2))^{(M-N)} \Gamma(M-N)}$$

¹¹The accuracy of our approximations are evaluated at the end of Appendix.

¹²The accuracy of this approximation increases as the ratio of DoFs between A and B, i.e., $\frac{M-N+1}{M}$, approaches one.

¹³It should be pointed out that the variance of the minimum *local* error is very small compared to that of $\|\check{\mathbf{v}}_b^{\text{virt}}\|_2^2$. We thus conclude that the operation of replacing the *local* error term by its expectation will lead a minimal effect.

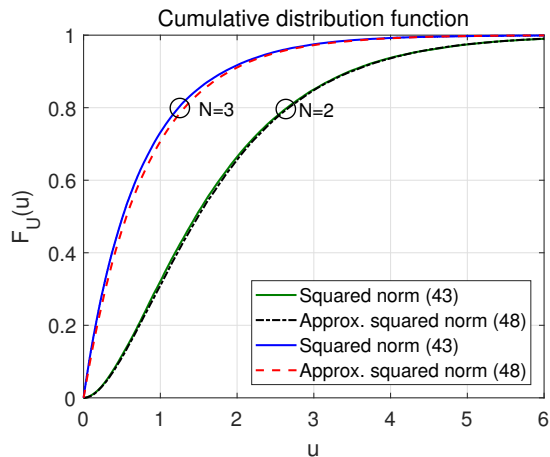


Fig. 9. CDF of squared norm of global effective vectors ($M = 4$).

$$= \frac{u^{M-N-1} e^{-u/e^2}}{\rho^{2(M-N)} \Gamma(M-N)}. \quad (49)$$

Finally, we evaluate the approximated *global* effective channel vectors by comparing their squared norm quantities. Based on the numerical results in Fig. 9, we conclude that the *global* effective channel vector is well approximated by (46). For the rest of sections, we use the approximated channel vector with the pdf defined in (49).

REFERENCES

- [1] A. Zanella, N. Bui, A. Castellani, L. Vangelista, and M. Zorzi, "Internet of things for smart cities," *IEEE Internet of Things Journal*, vol. 1, no. 1, pp. 22–32, Feb. 2014.
- [2] J. Lin, W. Yu, N. Zhang, X. Yang, H. Zhang, and W. Zhao, "A survey on internet of things: architecture, enabling technologies, security and privacy, and applications," *IEEE Internet of Things Journal*, vol. 4, no. 5, pp. 1125–1142, Oct. 2017.
- [3] C. Bockelmann, N. Pratas, G. Wunder, S. Saur, M. Navarro, D. Gregoratti, G. Vivier, E. D. Carvalho, Y. Ji, C. Stefanović, P. Popovski, Q. Wang, M. Schellmann, E. Kosmatos, P. Demestichas, M. Raceala-Motoc, P. Jung, S. Stanczak, and A. Dekorsy, "Towards massive connectivity support for scalable mMTC communications in 5G networks," *IEEE Access*, vol. 6, pp. 28 969–28 992, 2018.
- [4] X. Lin, J. Li, R. Baldemair, T. Cheng, S. Parkvall, D. Larsson, H. Koorapaty, M. Frenne, S. Falahati, A. Grövlén, and K. Werner, "5G new radio: unveiling the essentials of the next generation wireless access technology," *arXiv preprint arXiv:1806.06898*, 2018.
- [5] F. Boccardi, R. Heath, A. Lozano, T. Marzetta, and P. Popovski, "Five disruptive technology directions for 5G," *IEEE Communications Magazine*, vol. 52, no. 2, pp. 74–80, Feb. 2014.
- [6] T. Taleb and A. Kunz, "Machine type communications in 3GPP networks: potential, challenges, and solutions," *IEEE Communications Magazine*, vol. 50, no. 3, Mar. 2012.
- [7] P. Viswanath, D. Tse, and R. Laroia, "Opportunistic beamforming using dumb antennas," *IEEE Transactions on Information Theory*, vol. 48, no. 6, pp. 1277–1294, Jun. 2002.
- [8] W. Santipach and M. L. Honig, "Asymptotic performance of MIMO wireless channels with limited feedback," in *Proceedings of IEEE Military Communications Conference*, Oct. 2003.
- [9] D. J. Love, R. W. Heath, and T. Strohmer, "Grassmannian beamforming for multiple-input multiple-output wireless systems," *IEEE Transactions on Information Theory*, vol. 49, no. 10, pp. 2735–2747, Oct. 2003.
- [10] D. J. Love, R. W. Heath, W. Santipath, and M. L. Honig, "What is the value of limited feedback for MIMO channels?" *IEEE Communications Magazine*, vol. 42, no. 10, pp. 54–59, Oct. 2004.
- [11] J. Song, J. Choi, T. Kim, and D. J. Love, "Advanced quantizer designs for FDD-based FD-MIMO systems using uniform planar arrays," *IEEE Transaction on Signal Processing*, vol. 66, no. 14, pp. 3891–3905, Jul. 2018.
- [12] N. Jindal, "MIMO broadcast channels with finite rate feedback," *IEEE Transactions on Information Theory*, vol. 52, no. 11, pp. 5045–5059, Nov. 2006.
- [13] T. Yoo, N. Jindal, and A. Goldsmith, "Multi-antenna downlink channels with limited feedback and user selection," *IEEE Journal on Selected Areas in Communications*, vol. 25, no. 7, pp. 1478–1491, Sep. 2007.
- [14] N. Jindal, "Antenna combining for the MIMO downlink channel," *IEEE Transactions on Wireless Communications*, vol. 7, no. 10, pp. 3834–3844, Feb. 2008.
- [15] M. Zhao, J. Ryu, J. Lee, T. Quek, and S. Feng, "Exploiting trust degree for multiple-antenna user cooperation," *IEEE Transactions on Wireless Communications*, vol. 16, no. 8, pp. 4908–4923, Aug. 2017.
- [16] J. Chen, H. Yin, L. Cottatellucci, and D. Gesbert, "Feedback mechanisms for FDD massive MIMO with D2D-based limited CSI sharing," *IEEE Transactions on Wireless Communications*, vol. 16, no. 8, pp. 5162–5175, Aug. 2017.
- [17] J. Chung, C.-H. Hwang, K. Kim, and Y. K. Kim, "A random beamforming technique in MIMO systems exploiting multiuser diversity," *IEEE Journal on Selected Areas in Communications*, vol. 21, no. 5, pp. 848–855, Jun. 2003.
- [18] R1-103378, *Performance evaluations of Rel.10 feedback framework*, 3GPP TSG RAN WG1 #61 Std., May 2010.
- [19] R1-105011, *Way forward on 8Tx codebook for Rel.10 DL MIMO*, 3GPP TSG RAN WG1 #61 Std., Aug. 2010.
- [20] M. Kountouris, D. Gesbert, and T. Sälzer, "Enhanced multiuser random beamforming: dealing with the not so large number of users case," *IEEE Journal on Selected Areas in Communications*, vol. 26, no. 8, pp. 1536–1545, Oct. 2008.
- [21] M. Trivellato, F. Boccardi, and H. Huang, "On transceiver design and channel quantization for downlink multiuser MIMO systems with limited feedback," *IEEE Journal on Selected Areas in Communications*, vol. 26, no. 8, pp. 1494–1504, Oct. 2008.
- [22] J. Song, J. H. Lee, S. C. Kim, and Y. Kim, "Low-complexity multiuser MIMO downlink system based on a small-sized CQI quantizer," *EURASIP Journal on Wireless Communications and Networking*, vol. 2012, no. 1, pp. 1–15, Feb. 2012.
- [23] M. Sharif and B. Hassibi, "A comparison of time-sharing, DPC, and beamforming for MIMO broadcast channels with many users," *IEEE Transactions on Communications*, vol. 51, no. 1, pp. 11–15, Jan. 2007.
- [24] —, "On the capacity of MIMO broadcast channels with partial side information," *IEEE Transactions on Information Theory*, vol. 51, no. 2, pp. 506–522, Feb. 2005.
- [25] W. Shin, N. Lee, J.-B. Lim, C. Shin, and K. Jang, "Interference alignment through user cooperation for two-cell MIMO interfering broadcast channels," in *Proceedings of IEEE Global Telecommunications Conference*, Dec. 2010.
- [26] E. R. Hansen, *A table of series and products*. New Jersey: Prentice Hall, 1975.
- [27] H. David, *Order statistics*, 2nd ed. New York: John Wiley and Sons, 1980.
- [28] D. Gore, R. W. Heath, and A. Paulraj, "On performance of the zero forcing receiver in presence of transmit correlation," in *Proceedings of IEEE International Symposium on Information Theory*, 2002.
- [29] J. G. Proakis, *Digital communications*, 4th ed. McGraw-Hill, 2008.
- [30] R. J. Muirhead, *Aspects of multivariate statistical theory*. John Wiley & Sons, 2009.